



Article

Monoterpene-Containing Substituted Coumarins as Inhibitors of Respiratory Syncytial Virus (RSV) Replication

Tatyana M. Khomenko ¹, Anna A. Shtro ², Anastasia V. Galochkina ², Yulia V. Nikolaeva ², Galina D. Petukhova ², Sophia S. Borisevich ³ , Dina V. Korchagina ¹, Konstantin P. Volcho ^{1,*}  and Nariman F. Salakhutdinov ¹

¹ Department of Medicinal Chemistry, N.N. Vorozhtsov Novosibirsk Institute of Organic Chemistry, Acad. Lavrentjev Ave. 9, 630090 Novosibirsk, Russia; chomenko@nioch.nsc.ru (T.M.K.); korchaga@nioch.nsc.ru (D.V.K.); anvar@nioch.nsc.ru (N.F.S.)

² Laboratory of Chemotherapy for Viral Infections, Smorodintsev Research Institute of Influenza, Professor Popova Str., 15/17, 197376 St. Petersburg, Russia; anna.shtro@influenza.spb.ru (A.A.S.); nastiyagalochkina@yandex.ru (A.V.G.); ulechka.s89@gmail.com (Y.V.N.); galina.petukhova@influenza.spb.ru (G.D.P.)

³ Laboratory of Physical Chemistry, Ufa Chemistry Institute of the Ufa Federal Research Center, 71 Octyabrya pr., 450054 Ufa, Russia; monrel@mail.ru

* Correspondence: volcho@nioch.nsc.ru

Abstract: Respiratory syncytial virus (RSV) is a critical cause of infant mortality. However, there are no vaccines and adequate drugs for its treatment. We showed, for the first time, that O-linked coumarin–monoterpene conjugates are effective RSV inhibitors. The most potent compounds are active against both RSV serotypes, A and B. According to the results of the time-of-addition experiment, the conjugates act at the early stages of virus cycle. Based on molecular modelling data, RSV F protein may be considered as a possible target.

Keywords: coumarin; terpene; antiviral activity; cytotoxicity; respiratory syncytial virus; molecular modelling; F protein



Citation: Khomenko, T.M.; Shtro, A.A.; Galochkina, A.V.; Nikolaeva, Y.V.; Petukhova, G.D.; Borisevich, S.S.; Korchagina, D.V.; Volcho, K.P.; Salakhutdinov, N.F. Monoterpene-Containing Substituted Coumarins as Inhibitors of Respiratory Syncytial Virus (RSV) Replication. *Molecules* **2021**, *26*, 7493. <https://doi.org/10.3390/molecules26247493>

Academic Editor: Yuri Baukov

Received: 11 November 2021

Accepted: 9 December 2021

Published: 10 December 2021

Publisher's Note: MDPI stays neutral with regard to jurisdictional claims in published maps and institutional affiliations.



Copyright: © 2021 by the authors. Licensee MDPI, Basel, Switzerland. This article is an open access article distributed under the terms and conditions of the Creative Commons Attribution (CC BY) license (<https://creativecommons.org/licenses/by/4.0/>).

1. Introduction

Respiratory syncytial virus (RSV), which belongs to the Pneumoviridae family, is an enveloped negative-sense RNA virus with two major serotypes, A and B [1]. RSV infects the respiratory tract, causing annual epidemics during the cold season. Despite a relatively low variability of this virus, the immunity to it is unstable, which may cause repeated infections of the same individual throughout life. It usually causes a cold. Patients under the age of 2 years, especially those born prematurely or with a heart condition, as well as the elderly, develop different symptoms of respiratory syncytial infection [2–4]. These age groups present with involvement of not only the upper respiratory tract, but the lower respiratory tract as well, and develop severe bronchiolitis and pneumonia, which can lead to death. RSV is the most common cause of bronchiolitis and pneumonia in children younger than one year of age [5]. According to a meta-analysis carried out in 2010, the number of children who may die from this disease is estimated to be about 199,000 annually [6]. RSV-associated childhood respiratory illness has become a challenge since the summer of 2021, when the number of cases increased sharply, which may have been due to the relaxation of COVID-19 quarantine measures [7]. There is no vaccine for RSV. Therapy for respiratory syncytial infection is usually symptomatic. The only treatment option is a non-specific and poorly effective antiviral agent: ribavirin [8,9]. In addition, the monoclonal antibody Palivizumab is approved for prophylaxis, but it is expensive and only moderately effective at reducing hospitalization rates.

In recent decades, there has been significant progress in the identification of potential targets for RSV therapy and the search for low-molecular-weight inhibitors of RSV replication; the results of these studies were summarized in a review published

in 2019 [10]. Of particular interest are new low-molecular-weight agents against RSV, such as (perylene-3-ylethynyl)uracil derivative **1** [11], furanoxazine-fused benzimidazole **2** [12], and benzamide **3** [13] (Figure 1), which inhibit RSV replication by acting on cellular targets, as well as JNJ-53718678 [14] and sisunatovir [15], which are under second phase of clinical trials and are highly effective inhibitors of the fusion (F) protein. The F protein is essential for viral entry into the host cell.

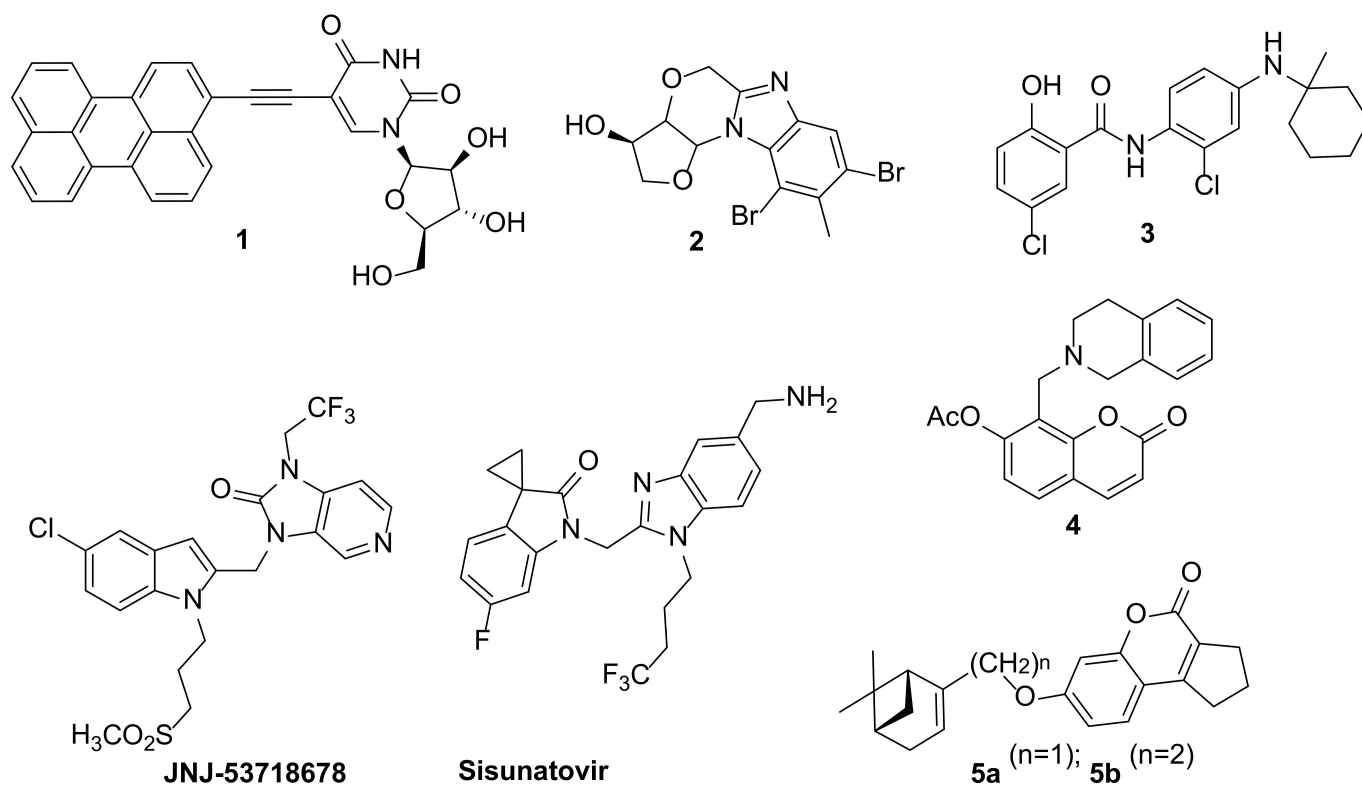


Figure 1. Known compounds with anti-RSV activity.

Many coumarin derivatives display a variety of biological activities [16–20], in particular antiviral activity [21–27]. Tetrahydroisoquinoline **4** is the only coumarin derivatives which exhibit anti-RSV activity [27]. Attachment of monoterpenoid fragments to parent molecules is known to significantly enhance their antiviral activity [28,29]. Recently, we have found that monoterpenoid-containing substituted 7-hydroxycoumarins effectively inhibit H1N1 influenza virus replication, with compound **5b** being most active [30]. Conjugate **5a** was found to exhibit the highest activity when added to infected cell culture at early stages of viral reproduction, probably due to the interaction with viral hemagglutinin. Replacement of the monoterpenoid moiety with a benzyl substituent led to a complete loss of antiviral activity. However, there are no data on RSV inhibitory activity of coumarin derivatives comprising a terpene moiety. In this study, we revealed the ability of monoterpenoid–coumarin conjugates to inhibit RSV replication and suggested a possible mechanism of their action.

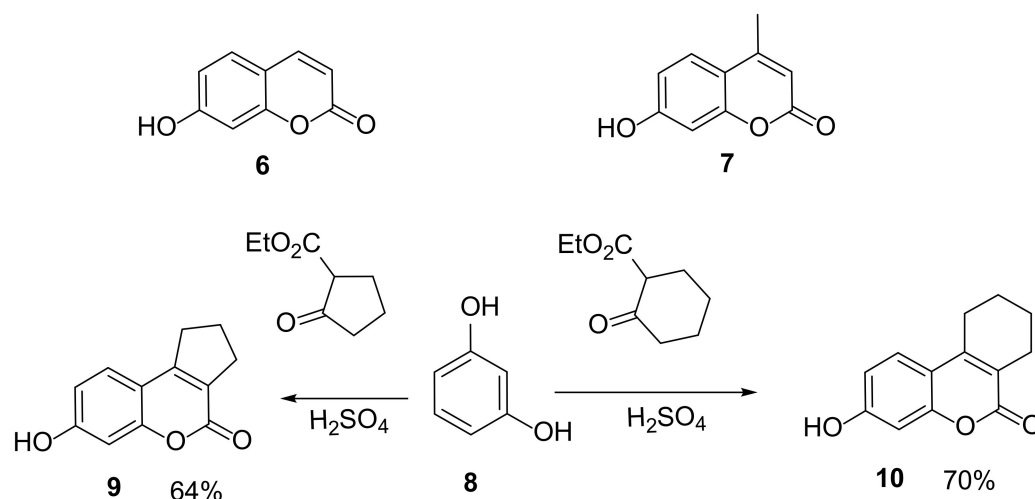
2. Results and Discussion

2.1. Chemistry

Our earlier study on the activity of monoterpenoid–coumarin conjugates against the influenza virus revealed that the structure and absolute configuration of a monoterpenoid moiety and the size of an annulated aliphatic ring had a significant effect on the antiviral activity. In addition, as the length of an aliphatic bridge between monoterpenoid and coumarin moieties increases from one to two CH_2 -groups, the antiviral activity enhances [30]. Given

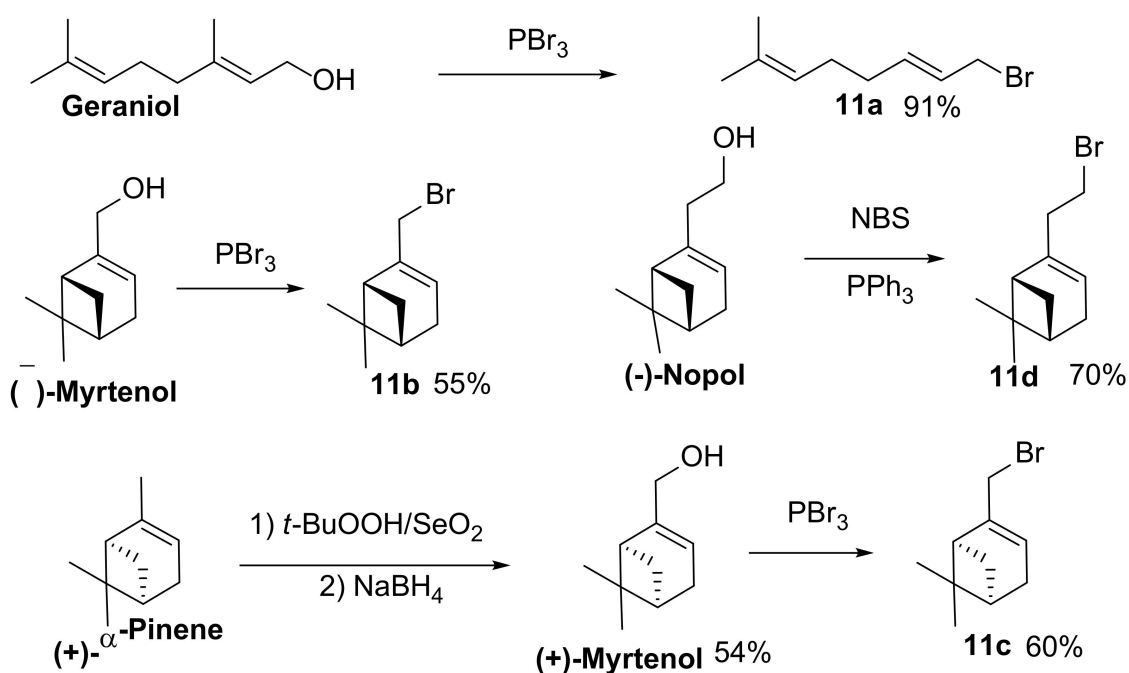
these data, in this study we synthesized a library of compounds that included both previously obtained coumarin–monoterpenoid hybrids [30,31] and new compounds with coumarin and monoterpene bicyclic fragments separated from each other by three or four CH₂-groups, as well as a number of nitrogen-containing coumarin derivatives with an NH₂-group instead of an OH-group.

7-Hydroxycoumarin derivatives were prepared from commercially available umbelliferone **6** and 4-methyl-7-hydroxycoumarin **7**, as well as coumarins **9** and **10** (Scheme 1) synthesized from resorcinol **8** according to [31].



Scheme 1. Synthesis of 7-hydroxycoumarins.

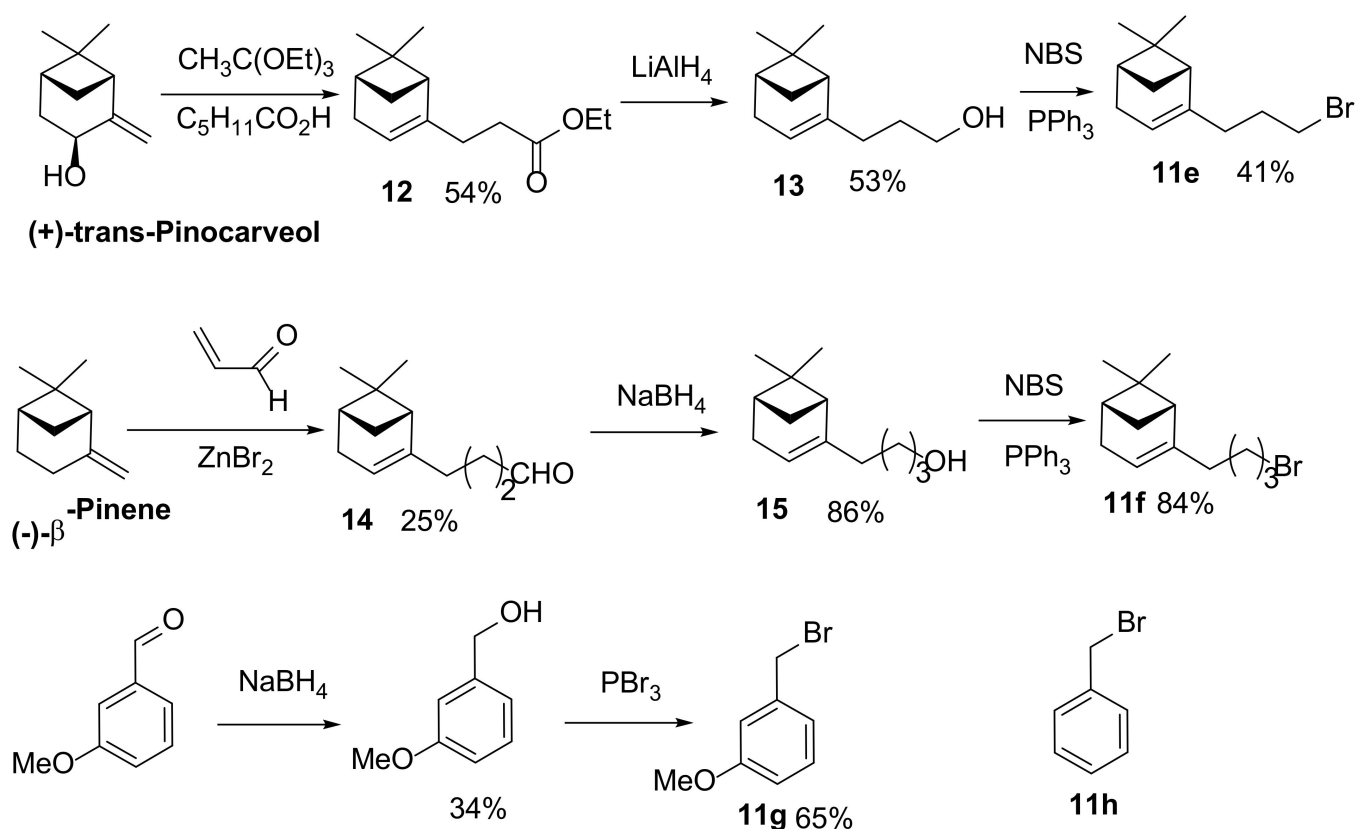
Bromides **11a–c** were synthesized in the reaction between appropriate alcohols and PBr₃ in accordance with [31], using geraniol, (–)-myrtenol, and (+)-myrtenol produced from (+)- α -pinene as starting monoterpenoids (Scheme 2). Nopol bromide **11d** was previously obtained by the method presented in [31] in a low yield; therefore, the NBS/PPh₃ system [32] was used to synthesize compound **11d**.



Scheme 2. Synthesis of monoterpene bromides **11a–d**.

Derivatives of (–)- α -pinene and its homologue (–)-nopol exhibited the highest activity against the influenza virus; therefore, we synthesized compounds containing an extended aliphatic chain and an (–)- α -pinene moiety. A homolog of nopol bromide **11d**, which contained an additional CH₂-group, was synthesized according to the following scheme: (+)-*Trans*-pinocarveol, which was prepared according to [33], reacted with triethyl orthoacetate in the presence of hexanoic acid to form ester **12**, which was then reduced by LiAlH₄ to alcohol **13** [34]. Bromide **11e** was prepared by treating alcohol **13** with NBS/PPh₃.

Another nopol bromide homolog containing two additional CH₂-groups, compound **11j**, was synthesized as follows (Scheme 3): (–)- β -Pinene reacted with acrolein in the presence of ZnBr₂ to form aldehyde **14** (conversion, 55%; yield after chromatography, 25%), which was reduced by NaBH₄ to alcohol **15** [35]. The interaction of alcohol **15** with NBS/PPh₃ resulted in bromide **11f** [35]. 1-(Bromomethyl)-3-methoxybenzene **11g** was synthesized from 3-methoxybenzaldehyde; in addition, benzyl bromide **11h** was used.

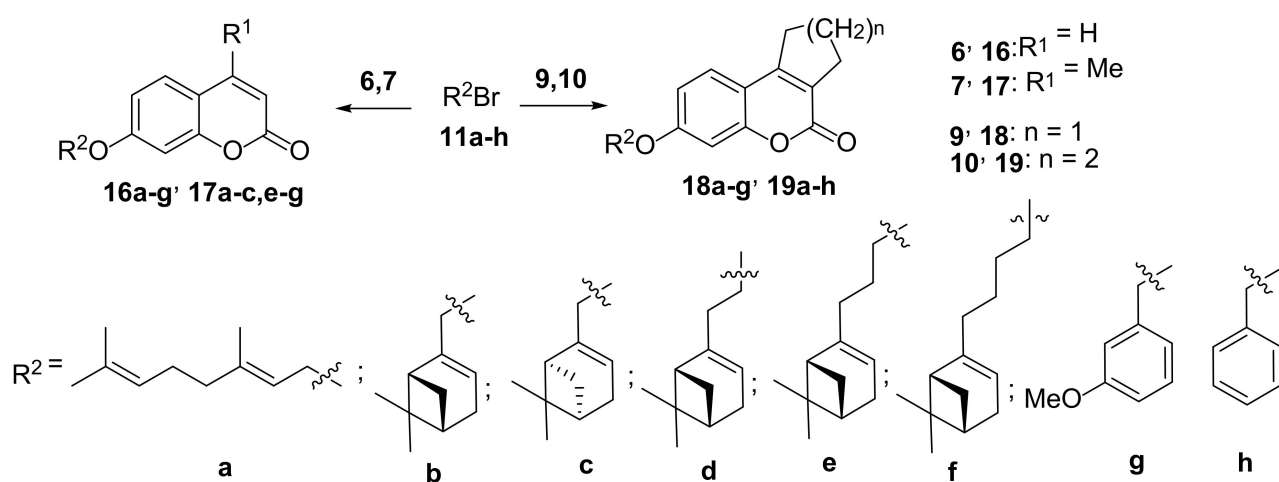


Scheme 3. Synthesis of bromides **11e–h**.

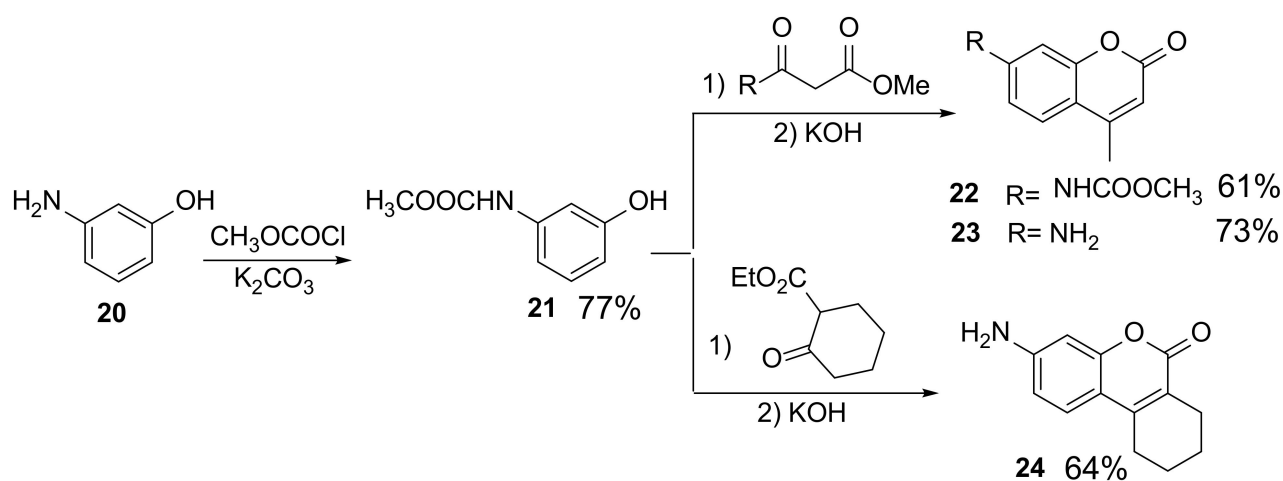
Auraptin **16a** and other coumarin derivatives **16–19** were prepared in the reaction of 7-hydroxycoumarins **6–10** with appropriate bromides **11** (Scheme 4), as described elsewhere [30]. The products were purified by recrystallization or column chromatography (yields 24–80%). The reaction of nopyl bromide **11d** with methylcoumarin **7** failed due to the formation of a complex reaction mixture with a high resinification level.

7-Aminocoumarins **23** and **24** were synthesized according to the method presented in [36], starting from 3-aminophenol **20**, via intermediate compound **21**, and its interaction with the appropriate ketoesters (Scheme 5).

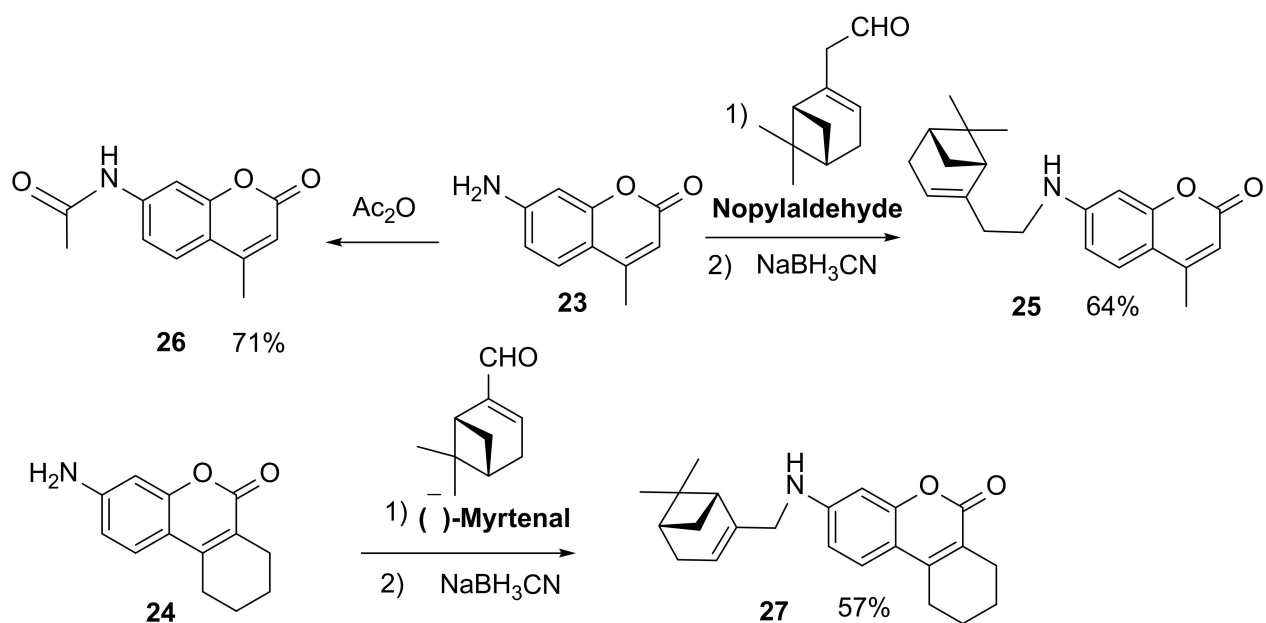
Furthermore, compound **23** reacted with (–)-nopol aldehyde, and on reduction with NaBH₃CN, produced secondary amine **25**. In addition, acylation of amine **23** with acetic anhydride led to acetamide **26** [37]. Similarly to compound **25**, amine **27** was synthesized from amine **24** and (–)-myrtenal (Scheme 6).



Scheme 4. Synthesis of substituted coumarins 16–19.



Scheme 5. Synthesis of aminocoumarins 23 and 24.



Scheme 6. Synthesis of aminocoumarin derivatives 25–27.

2.2. Biology

2.2.1. Cytotoxicity Test

The cytotoxicity was tested using a standard MTT-test (detailed below in Section 3.2.1). A series of 2-fold dilutions of compounds was made; then, each dilution was added to 24 h old cell monolayer, after which, cells were incubated for 24 h. Cell viability was assessed by adding the MTT solution. Based on the data obtained, the CC_{50} was calculated.

2.2.2. Antiviral Activity

The antiviral activity against the respiratory syncytial virus was assessed by adding a series of 3-fold dilutions of test compounds, followed by addition of the virus in a series of 10-fold dilutions. Cells were incubated for 1 h; then, the virus was washed out and compounds were added again. Cell were incubated for 6 days, after which the viral presence was investigated, using the ELISA method.

The virus titer was calculated using the Reed and Muench method.

The obtained results are shown in Table 1. Compounds were considered promising with a selectivity index of 10 or higher.

Table 1. Antiviral activity and cytotoxicity of compounds 16–18, 25–27 against RSV A and B.

Compound	R	CC_{50}^a , μM	RSV A		RSV B	
			IC_{50}^b , μM	SI^c	IC_{50} , μM	SI^c
16a		58.7 ± 7.6	6.7 ± 0.8	7.9	10.7 ± 2.1	5.5
16b		113 ± 25.6	>111	<1	34.4 ± 1.7	3.3
16c		307.1 ± 34.6	27 ± 1.8	11.4	18.5 ± 0.9	16.8
16d		25.8 ± 1.6	2.9 ± 0.67	8.9	23.5 ± 0.7	1.1
16e		24.7 ± 6.7	>25	<1	14.8 ± 0.9	1.7
16f		121.1 ± 24.5	2.5 ± 0.87	64.6	d.n.t. ^d	-
16g		1204.4 ± 204	41.6 ± 3.2	29.9	37.6 ± 7.4	32
17a		483.4 ± 23.6	46.7 ± 8.7	10.3	52.4 ± 3.4	9.2
17b		795.7 ± 28.9	29 ± 3.2	27.4	241 ± 41	3.3
17c		116 ± 23.6	1.3 ± 0.75	90	4.7 ± 0.9	24.7
17e		26.6 ± 12.3	12.4 ± 2.1	2.1	5 ± 1.7	5.3
17f		658.2 ± 54.6	13.9 ± 1.6	62.1	20.1 ± 3.2	32.7
17g		172 ± 21.1	>60.7	3	>185.6	<1.2

Table 1. Cont.

Compound	R	CC ₅₀ ^a , μM	RSV A		RSV B	
			IC ₅₀ ^b , μM	SI ^c	IC ₅₀ , μM	SI ^c
18a		26.6 ± 12.3	>26	<1	15.1±3.4	1.8
18b		13.4 ± 4.6	>13	<1	>13	0.9
18c		416.2 ± 32.9	4.1 ± 0.78	100	5.1±1.0	81.6
18d		408.1 ± 56.1	>400	<1	408.6	<1
18e		66.7 ± 23.1	4.1 ± 0.7	18.3	24.7 ± 5.3	2.7
18f		47.3 ± 12.7	50.2 ± 13.2	1	10 ± 1.7	4.7
18g		37.2 ± 9.8	>37	<1	21.7 ± 2.7	1.8
19a		51.1 ± 11.3	0.57 ± 0.2	90	0.6±0.1.	85.2
19b		333.9 ± 56.8	107.6 ± 13.5	3.1	60.5 ± 11.6	5.5
19c		379.5 ± 29.4	5.1 ± 1.1	77	4.9 ± 0.6	78.2
19d		21.9 ± 11.8	0.6 ± 0.13	40	0.82±0.1	26.7
19e		13.2 ± 4.8	6.1 ± 2.1	2.2	>13	<1
19f		718.4 ± 21.9	15.3 ± 1.8	57.9	8.2 ± 0.83	88.1
19g		930.5 ± 56.9	81.8 ± 3.3	11.4	19.8±1.7	46.9
19h		31.3 ± 7.4	>31	<1	5.2 ± 0.69	6
25		355,6 ± 12,7	33.7 ± 7.6	10.5	114.9 ± 16.7	3.1
26		84,3 ± 11,7	6.2 ± 1.2	14.5	>84	<0.9
27		53,5 ± 10,9	51.5 ± 5.4	1	>53	<0.9
Ribavirin		>4095	31.1 ± 6.7	131.6	54.5±5.9	75.1

^a CC₅₀ is the median cytotoxic concentration, i.e., the concentration causing 50% cell death. ^b IC₅₀ is the 50% inhibiting concentration, i.e., the concentration causing a 50% decrease in virus replication. ^c SI is the selectivity index, which is the CC₅₀/IC₅₀ ratio. CC₅₀'s and IC₅₀'s are presented as mean ± standard deviation. The values are calculated from three independent experiments. ^d d.n.t.—did not test.

At the first stage, all the prepared compounds were tested for their ability to inhibit the replication of RSV A. Aurapten **16a**, containing an acyclic monoterpene substituent, exhibited high activity against RSV A in the lower micromolar range, but its selectivity index was less than 8 due to high cytotoxicity. Among compounds **16b,c** containing an α -pinene fragment, only compound **16c**, derived from (+)- α -pinene, exhibited noticeable activity, with the selectivity index exceeding 11. Elongation of the hydrocarbon chain from **16b** to compounds **16d–f** led to a nonlinear change in the biological properties: high antiviral activity was exhibited by compounds with one (**16d**) and three (**16f**), but not two (**16e**) additional CH_2 -groups. Due to its lower cytotoxicity, compound **16f** displayed the best selectivity index, about 65, among monoterpene–coumarin conjugates of this type. Coumarin derivative **16g**, containing an aromatic substituent, showed a high selectivity index (30), which was related to its low cytotoxicity, rather than its high activity.

Among 4-methylcoumarin derivatives **17**, compound **17c**, containing an (+)- α -pinene moiety, exhibited high activity in the submicromolar range, whereas its (–)-isomer was 20-fold less active. Compound **17c** had a high selectivity index of 90. Elongation of the hydrocarbon chain (a compound with one additional CH_2 -group was not prepared due to the formation of a complex reaction mixture) did not affect the activity much; it was almost the same, similarly to toxicity. The less cytotoxic compound **17c** had a selectivity index of 62. Compound **17g**, containing an aromatic substituent, did not display significant antiviral activity.

Investigation of the biological properties of compound **18**, comprising a cyclopentane ring annulated with a coumarin moiety, showed that (+)- α -pinene derivative **18c** with a selectivity index of 100 exhibited the highest activity and moderate toxicity. The other compounds were either toxic (**18a,b,e–g**) or inactive (**18d**); only compound **18e** had a noticeable selectivity index of 18.

Among coumarin **19**, containing an annulated cyclohexane ring, the highest activity was exhibited by compounds **19a** and **19d**, which were derived from geraniol and nopol, respectively. High selectivity indices were also displayed by compounds **19c** and **19f**, which were both less active and less toxic. Coumarin derivative **19g**, containing a methoxybenzyl substituent, had a selectivity index of more than 10, which was due to its low cytotoxicity. Removal of the methoxy group from the aromatic ring in compound **19h** led to a sharp increase in its toxicity.

Amine **25** showed significant activity and moderate toxicity, which resulted in a selectivity index of more than 10. Transition to acetamide **26** led to a loss of the antiviral effect. Compound **27** was almost one order of magnitude more active and significantly more toxic than amine **25**, with the selectivity index being about 15. Compound **27** was much more active than its oxygen-containing analog **19b**, which substantiates further research regarding the synthesis of N-linked monoterpene–coumarin conjugates and the investigation of their anti-RSV activity.

A significant portion of the prepared coumarin derivatives were tested for their ability to inhibit RSV replication. Among the compounds tested, **16c,g**, **17c,f**, **18c**, **19a,c,d**, and **19f** had a selectivity index of more than 10, with the last two being most active. In general, activity of O-linked coumarin–monoterpene conjugates against RSV type B was similar to that against RSV type A, which indicates that the antiviral activity of these compounds lacks type specificity. At the same time, 7-aminocoumarin derivatives demonstrated some activity against RSV type A, but not type B. Among compounds with similar SI against both RSV types, **19c** was chosen to investigate a possible action mechanism.

To elucidate action mechanisms of the most active compounds, we performed an experiment using the time-of-addition method. Compound **19c** was added to the cells with replicating virus at different time points corresponding to different stages of viral life cycle. The results are shown in Figure 2.

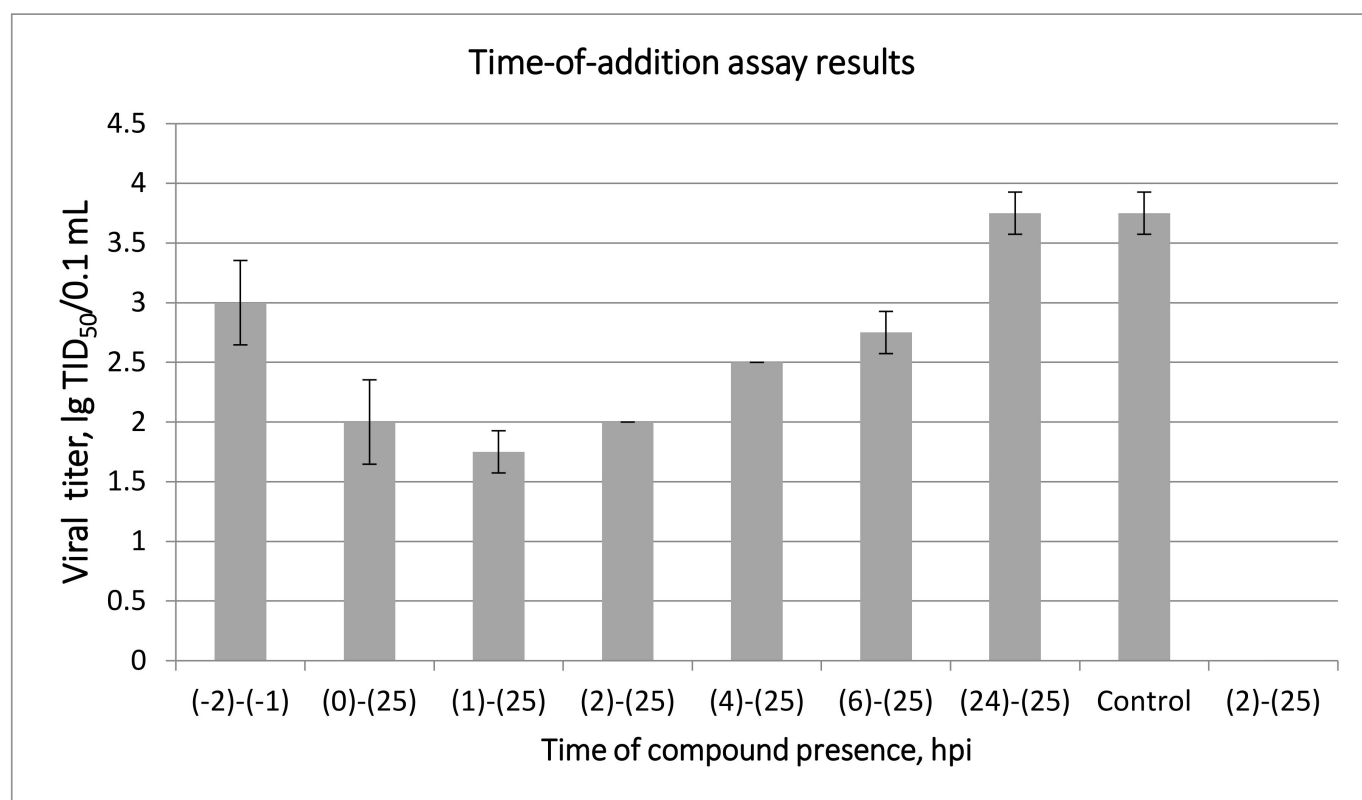


Figure 2. Activity of **19c** against RSV A according to time-of-addition experiment.

According to the data presented in Figure 2, compound **19c** reduces the virus titer at all time points, except for prophylactic use 2 h before virus entry into cells and late introduction after 24 h. This means that action of the compound occurred within 0–6 h after infection. A slight decrease in the virus titer was also noted at time points 2 and 4. Our data suggest that the target of **19c** may be the surface F and/or G proteins, viroporin SH, and, probably, L protein (its fragment responsible for transcription).

2.3. Molecular Modeling Study

According to the results of the time-of-addition experiment, the surface F protein may be considered a potential biological target. In addition, the pharmacophore features of the inhibitor of F-protein sisunatovir and compounds **19c**, **19f**, and **19h** are similar. In all cases, there are hydrophobic parts capable of hydrophobic intermolecular contacts, and donors and acceptors of hydrogen bonds (more details are presented in the Supplementary Materials).

We suggest that compounds **19c**, **19f**, and **19h** can bind to a fusion peptide region [38,39] (Figure 3A), similarly to sisunatovir [15] (Figure 3B). Several functional amino acids are located in the binding site of potential entry inhibitors (Figure 3A). The red segment in Figure 3 is a part of the fusion peptide (137–140 amino acids), and the yellow segment corresponds to amino acids of the membrane anchor. Entry inhibitors can interact with these amino acids and inhibit the conformational transition from a pre- to post-fusion conformation. The coumarin moiety of compounds **19c**, **19f**, and **19h** occurs in a cavity surrounded by phenylalanines and forms π – π stacking interactions with them (Figure 3C,D). The terpene fragment of **19c** and **19f** occurs in a hydrophobic cavity composed of amino acids of the fusion peptide region (Figure 3C,E). The aromatic part of **19h** cannot be placed into the cavity due to a short linker between it and the coumarin fragments (Figure 3D). Compound **19h** forms intramolecular interactions with amino acids of the membrane anchor.

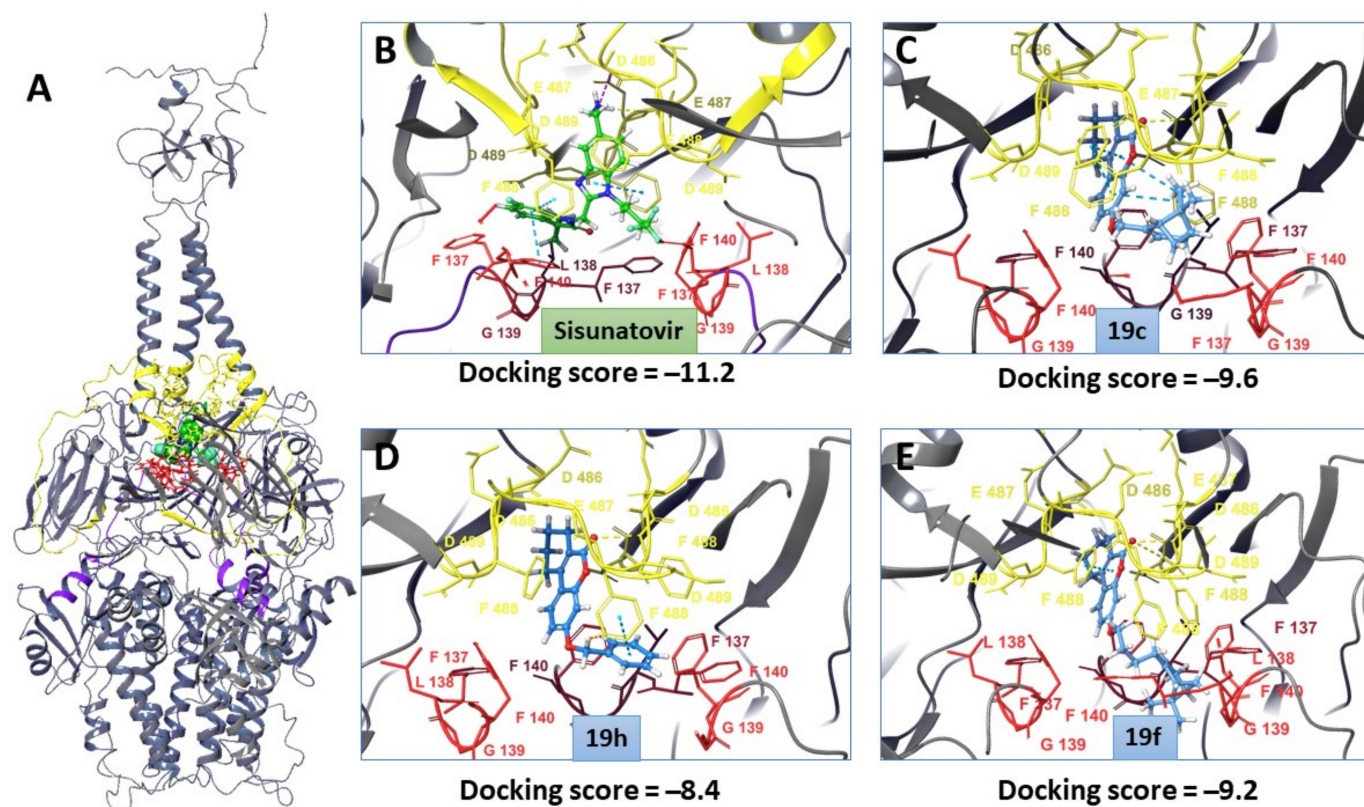


Figure 3. Structure of the RSV F-protein: (A) structure corresponds to PDB [40] code 7LVW [39]: fusion peptide region is presented in violet secondary structure (137–157 amino acids); functional residues (137–140) are shown in red; amino acids of the membrane anchor are shown in yellow (amino acids 454–499); the green molecule is sisunatovir [15]; (B) sisunatovir in the binding site; (C–E) positions of possible entry inhibitors (19c, 19f, and, 19h). π - π stacking interactions are denoted by blue dotted lines; H-bonds and salt bridges are denoted by yellow and violet lines, respectively.

Docking scores shown in Figure 3 may be considered as a parameter that characterizes the affinity of compounds to the binding site. The best positions are shown in Figure 3. The best ligand position was chosen based on the clustering energy and formation energy of the ligand–protein complex. For more energy parameters, see the Supplementary Materials. Affinity values of lead compounds have a slightly higher value than those for sisunatovir. Compound 19h had the lowest affinity. These results correlate with experimental data (Table S1). Thus, RSV F protein may be considered as a possible target.

3. Materials and Methods

3.1. Chemistry

3.1.1. General Chemical Methods

Reagents and solvents were purchased from commercial suppliers (Sigma-Aldrich, Acros, Japan) and used as received. GC-MS: Agilent 7890A gas chromatograph equipped with an Agilent 5975C quadrupole mass spectrometer as a detector; quartz column HP-5MS (copolymer 5%–diphenyl–95%–dimethylsiloxane) of length 30 m, internal diameter 0.25 mm and stationary phase film thickness 0.25 μ m. Optical rotation: polAAR 3005 spectrometer. ^1H and ^{13}C NMR: Bruker DRX-500 apparatus at 500.13 MHz (^1H) and 125.76 MHz (^{13}C) and Bruker Avance—III 600 apparatus at 600.30 MHz (^1H) and 150.95 MHz (^{13}C), J in Hz; structure was determined by analyzing the ^1H NMR spectra, including ^1H – ^1H double resonance spectra and ^1H – ^1H 2D homonuclear correlation (COSY, NOESY), J -modulated ^{13}C NMR spectra (JMOD), and ^{13}C – ^1H 2D heteronuclear correlation with one-bond (C–H COSY, $^1J(\text{C},\text{H}) = 160$ Hz, HSQC, $^1J(\text{C},\text{H}) = 145$ Hz) and long-range spin–spin coupling constants (C–H COSY, $^1J(\text{C},\text{H}) = 160$ Hz, HSQC, $^1J(\text{C},\text{H}) = 145$ Hz).

HR-MS: DFS Thermo Scientific spectrometer in a full scan mode (15–500 m/z , 70 eV electron impact ionization, direct sample administration).

Spectral and analytical investigations were carried out at the Collective Chemical Service Center of the Siberian Branch of the Russian Academy of Sciences. All product yields are given for pure compounds purified by recrystallization from ethanol or isolated by column chromatography (SiO_2 ; 60–200 μ ; Macherey-Nagel). The purity of the target compounds was determined by GC-MS methods. All of the target compounds reported in this paper had a purity of no less than 95%.

3.1.2. Synthesis of Coumarins **9**, **10**

Syntheses were carried out from resorcinol **5** and appropriate β -ketoesters **6**, **7**, in accordance with [31]. Concentrated H_2SO_4 (5 mL, 94 mmol) was added dropwise to cooled (0–5 °C) solution of resorcinol **8** (45 mmol) and appropriate β -ketoesters (45 mmol) in dry ethanol (15 mL), with vigorous stirring. The mixture was stirred until it congealed, left overnight at r.t., and poured into ice water (150 mL). The resulting solid was filtered off and crystallized from ethanol–water (75%). The yields of **9**, **10** were 64% and 70%, respectively.

3.1.3. Synthesis of Bromides **11a–c,g**

(+)-Myrtenal was synthesized according to the procedure presented in [41] by the oxidation of (+)- α -pinene using a $t\text{-BuOOH}/\text{SeO}_2$ system with a 57% yield.

(+)-Myrtenol was synthesized from the corresponding aldehyde via reduction to alcohols with NaBH_4 , as described above. NaBH_4 (10.3 mmol) was added to a cooled (0–5 °C) solution of 10.3 mmol of the appropriate aldehyde in methanol (20 mL), and the reaction mixture was stirred for 3 h at room temperature. Then, 5% aqueous HCl was added to obtain a pH of 4–5. The solvent was distilled, and the product was extracted using ether and dried with Na_2SO_4 . The solvent was evaporated; the resulting alcohol (54% yield) was used in the synthesis without purification.

(3-Methoxyphenyl)methanol was synthesized from 3-methoxybenzaldehyde via a reaction with NaBH_4 , as described above (yield: 34%).

Bromide **11a** was synthesized from geraniol via the reaction with PBr_3 [30].

PBr_3 (8.9 mmol) was added to cooled (0–5 °C) solution of geraniol (26.7 mmol) in dry ether (30 mL), and the reaction mixture was stirred for 2 h at r.t. Saturated aqueous NaHCO_3 was added, and the product was extracted with ether. The extracts were washed with brine, dried with Na_2SO_4 , and evaporated.

Additional bromides **11b,c,g** were synthesized as described above. Compounds **11a–c,g** (with yields of 91%, 55%, 60% and 65%, respectively) were sufficiently pure and used for the next step without purification.

3.1.4. Synthesis of Bromide **11d**

Bromide **11d** was synthesized from (–)-nopol via reaction with NBS– PPh_3 , as described in [32].

Triphenylphosphine (2.0 equiv., 6.1 g, 23 mmol) was dissolved in dry DCM (23 mL) under argon. *N*-bromosuccinimide (NBS) (2.0 equiv., 4.2 g, 23 mmol) was added to this solution in small portions over 5 min in an ice-water bath. Subsequently, the resulting deep red mixture was stirred at room temperature for 30 min. Then, pyridine (1 mL) was added, and the color turned reddish-brown. (–)-Nopol (1.0 equiv., 2.0 mL, 12 mmol) was added to the mixture dropwise over 10 min. The reaction mixture was stirred overnight at room temperature. Later, the mixture was diluted with hexane (40 mL) and filtered through a silica gel plug. Then, the reaction flask was stirred with EtOAc –hexane (1:1, 40 mL) and filtered through the silica gel plug. Later, it was concentrated in vacuo and the crude residue was purified by chromatography on SiO_2 (hexane) to obtain bromide **11d** (2.3 g, 70% yield).

3.1.5. Synthesis of Bromide 11e

Bromide **11e** was synthesized from alcohol **13** via a reaction with NBS–PPh₃, as described for **11d** (the yield of **11e**–41%). Alcohol **13** was obtained by the reduction of ether **12**, synthesized from (+)-*trans*-pinocarveol [34] with LiAlH₄.

A mixture of (+)-*trans*-pinocarveol (2.45 g, 16 mmol; obtained by the oxidation of β-pinene with *t*-BuOOH in the presence of SeO₂, in accordance with [33]), triethyl orthoacetate (3.93 g, 24 mmol), and hexanoic acid (0.25 g, 2.4 mmol) was heated for 6 h at 150 °C. The mixture was then diluted with Et₂O (150 mL) and washed successively with sat. aq. NaHCO₃ soln. and H₂O, dried with Na₂SO₄, and evaporated. Compound **12** was purified by column chromatography on SiO₂, eluent–hexane–ethyl acetate (1.92 g, yield 54%).

A solution of **12** (2.22 g, 10 mmol) in Et₂O (10 mL) was added dropwise to a suspension of LiAlH₄ (2.1 g, 55 mmol) in refluxing Et₂O (20 mL). After 1 h at r.t., the mixture was cooled to 0 °C, and H₂O (2 mL), 15% aq. NaOH soln. (2 mL), and then H₂O (3 mL) were added. After 30 min, the mixture was filtered and evaporated. Compound **13** was purified by column chromatography on SiO₂, eluent–hexane–ethyl acetate (1.40 g, yield 78%).

3.1.6. Synthesis of Bromide 11f

Aldehyde **14**, obtained according to [35], was reduced to alcohol **15** by NaBH₄ (yield: 86%). The OH group of alcohol **15** was replaced by Br using NBS–PPh₃ (yield **11f**: 84%). Then, 100 mL Et₂O, acrolein (8.6 g, 154 mmol) and (–)-β-pinene (14.5 g, 107 mmol) were added to a solution of anhydrous ZnBr₂ (4.3 g, 19 mmol). The solution was stirred for 48 h at 25 °C. Then, it was poured into water (200 mL) and filtered by suction to remove zinc salts. The ether layer was separated, and the aqueous layer was extracted with 2 × 50 mL Et₂O. The combined ether layers were dried and evaporated. Compound **14** was purified by column chromatography on SiO₂, eluent–hexane–CHCl₃ (30%) (**14**: 3.76 g, yield 25%, unreacted (–)-β-pinene–3.13 g).

3.1.7. Synthesis of Compounds 16a–g, 17a–c,e–g, 18a–g and 19a–g

Compounds **16a–d,g**, were synthesized from coumarin **6** and the corresponding bromides **11a–d,g** with the use of DBU and DMF, in accordance with [30].

DBU (1.0 mmol) and the corresponding bromides **11a–d,g** (0.75 mmol) were added to compound **1** (0.5 mmol) in dry DMF (5 mL) at r.t. under stirring. The reaction mixture was stirred at r.t. for 15 min, and then heated at 60 °C for 5 h. H₂O (15 mL) was added, and the product was extracted with ethyl acetate. The extracts were washed with brine, dried with Na₂SO₄, and evaporated.

Compounds **16e,f**, **16e,f**, **17e,f** and **18e,f** were synthesized as above.

Compounds **16a**, **17a**, and **18a** were synthesized from coumarins **6,7,9** and geranyl bromide **11a** with the use K₂CO₃ and ethanol, in accordance with [31].

K₂CO₃ (1.0 mmol) and geranyl bromide **11a** (0.75 mmol) were added to corresponding compounds **5–7** (0.5 mmol) in dry ethanol (5 mL) at r.t. under stirring. The reaction mixture was stirred at r.t. for 15 min, and then heated at 60 °C for 5 h. The hot solution was filtered; the filtrate was kept at –18 °C for 48 h.

Compounds **17a–c,g**, **18a–d,g**, and **19a–d,g** were synthesized from coumarins **7,9,10** and corresponding bromides **11a–d,g** with the use K₂CO₃ and ethanol, as described above.

¹H NMR spectra of **16a–d,g**, **17a–c,g**, **18a–d,g**, and **19a–d,g** coincided with the corresponding spectra published in the literature [30,31].

Products **16a–g**, **17a–c,e–g**, **18a–g**, and **19a–g** were isolated in the individual form: (a) by recrystallization from ethanol; or (b) by column chromatography on a silica gel, eluent–hexane, solution containing from 25% to 100% chloroform in hexane, ethanol.

7-(3-((1*R*,5*S*)-6,6-Dimethylbicyclo[3.1.1]hept-2-en-2-yl)propoxy)-2*H*-chromen-2-one (**16e**). Yield: 58%, method **b**. M.p. 75 °C. [α]_D^{24.5} = –19.4 (*c* = 1.40, CHCl₃). HRMS: 324.1714 ([M]⁺, *m/z* calcd for C₂₁H₂₄O₃ 324.1720). ¹H-NMR (CDCl₃, δ_H): 0.80 (s, 3H-C(21)); 1.11 (d, 1H, ²J = 8.5, H_{anti} H-C(19)); 1.24 (s, 3H-C(20)); 1.77–1.89 (m, 2H, 2H-C(11)); 2.00 (ddd, 1H, J_{18,16} = J_{18,19sin} = 5.6, J_{18,14} = 1.4, H-C(18)); 2.03–2.11 (m, 3H, 2H-C(12)), 1H-C(16)); 2.15

(dm, 1H, $^2J = 17.5$, H-C(15)); 2.22 (dm, 1H, $^2J = 17.5$, H'-C(15)); 2.34 (ddd, 1H, $^2J = 8.5$, $J_{19\text{sin},16} = J_{19\text{sin},18} = 5.6$, $H_{\text{sin-C(19)}}$); 3.94–3.98 (m, 2H, 2H-C(10)); 5.18–5.22 (m, 1H, H-C(14)); 6.19 (d, 1H, $J_{3,4} = 9.5$, H-C(3)); 6.75 (d, 1H, $J_{9,7} = 2.4$, H-C(9)); 6.79 (dd, 1H, $J_{7,6} = 8.5$, $J_{7,9} = 2.4$, H-C(7)); 7.32 (d, 1H, $J_{6,7} = 8.5$, H-6); 7.59 (d, 1H, $J_{4,3} = 9.5$, H-4). $^{13}\text{C-NMR}$ (CDCl_3 , δ_{C}): 155.74 (s, C(1)); 161.05 (s, C(2)); 112.72 (d, C(3)); 143.27 (d, C(4)); 112.21 (s, C(5)); 128.53 (d, C(6)); 112.78 (d, C(7)); 162.24 (s, C(8)); 101.15 (d, C(9)); 68.11 (t, C(10)); 26.42 (t, C(11)); 32.83 (t, C(12)); 146.90 (s, C(13)); 116.61 (d, C(14)); 31.09 (t, C(15)); 40.66 (d, C(16)); 37.78 (s, C(17)); 45.58 (d, C(18)); 31.53 (t, C(19)); 26.14 (q, C(20)); 21.02 (q, C(21)).

7-(4-((1R,5S)-6,6-Dimethylbicyclo[3.1.1]hept-2-en-2-yl)butoxy)-2H-chromen-2-one (16f).

Yield: 80%, method b. $[\alpha]_{589}^{22} = -9.0$ ($c = 1.78$, CHCl_3). HRMS: 337.1793 ($[\text{M-H}]^+$, m/z calcd for $\text{C}_{22}\text{H}_{25}\text{O}_3$ 337.1798). $^1\text{H-NMR}$ (CDCl_3 , δ_{H}): 0.80 (s, 3H-C(22)); 1.11 (d, 1H, $^2J = 8.5$, $H_{\text{anti-C(20)}}$); 1.24 (s, 3H-C(21)); 1.42–1.56 (m, 2H, 2H-C(12)); 1.74–1.81 (m, 2H, 2H-C(11)); 1.95–2.02 (m, 3H, 2H-C(13)), 1H-C(19)); 2.02–2.08 (m, 1H, H-C(17)); 2.15 (dm, 1H, $^2J = 17.4$, H-C(16)); 2.22 (dm, 1H, $^2J = 17.4$, H'-C(16)); 2.32 (ddd, 1H, $^2J = 8.5$, $J_{20\text{sin},17} = J_{20\text{sin},19} = 5.6$, $H_{\text{sin-C(20)}}$); 3.98 (t, 2H, $J_{10,11} = 6.5$, 2H-C(10)); 5.16–5.20 (m, 1H, H-C(15)); 6.20 (d, 1H, $J_{3,4} = 9.5$, H-C(3)); 6.76 (d, 1H, $J_{9,7} = 2.4$, H-C(9)); 6.79 (dd, 1H, $J_{7,6} = 8.6$, $J_{7,9} = 2.4$, H-C(7)); 7.32 (d, 1H, $J_{6,7} = 8.6$, H-C(6)); 7.59 (d, 1H, $J_{4,3} = 9.5$, H-C(4)). $^{13}\text{C-NMR}$ (CDCl_3 , δ_{C}): 155.77 (s, C(1)); 161.07 (s, C(2)); 112.74 (d, C(3)); 143.26 (d, C(4)); 112.22 (s, C(5)); 128.53 (d, C(6)); 112.79 (d, C(7)); 162.26 (s, C(8)); 101.21 (d, C(9)); 68.38 (t, C(10)); 28.56 (t, C(11)); 23.32 (t, C(12)); 36.31 (t, C(13)); 147.68 (s, C(14)); 116.14 (d, C(15)); 31.12 (t, C(16)); 40.73 (d, C(17)); 37.78 (s, C(18)); 45.60 (d, C(19)); 31.52 (t, C(20)); 26.19 (q, C(21)); 21.05 (q, C(22)).

7-(3-((1R,5S)-6,6-Dimethylbicyclo[3.1.1]hept-2-en-2-yl)propoxy)-4-methyl-2H-chromen-2-one (17e). Yield: 49%, method a. M.p. 86 °C. $[\alpha]_{589}^{24.5} = -19.5$ ($c = 0.65$, CHCl_3). HRMS: 337.1796 ($[\text{M-H}]^+$, m/z calcd for $\text{C}_{22}\text{H}_{25}\text{O}_3$ 337.1798). $^1\text{H-NMR}$ (CDCl_3 , δ_{H}): 0.81 (s, 3H-C(22)); 1.13 (d, 1H, $^2J = 8.5$, $H_{\text{anti-C(20)}}$); 1.25 (s, 3H-C(21)); 1.78–1.90 (m, 2H, 2H-C(12)); 2.01 (ddd, 1H, $J_{19,17} = J_{19,20\text{sin}} = 5.6$, $J_{19,15} = 1.3$, H-C(19)); 2.04–2.12 (m, 3H, 2H-C(13)), 1H-C(17)); 2.17 (dm, 1H, $^2J = 17.5$, H-C(16)); 2.23 (dm, 1H, $^2J = 17.5$, H'-C(16)); 2.35 (ddd, 1H, $^2J = 8.5$, $J_{20\text{sin},17} = J_{20\text{sin},19} = 5.6$, $H_{\text{sin-C(20)}}$); 2.37 (d, 3H, $J_{10,3} = 0.8$, 3H-C(10)); 3.97 (t, 2H, $J_{11,12} = 6.5$, 2H-C(11)); 5.20–5.23 (m, 1H, H-C(15)), 6.09 (q, 1H, $J_{3,10} = 0.8$, H-C(3)); 6.77 (d, 1H, $J_{9,7} = 2.5$, H-C(9)); 6.82 (dd, 1H, $J_{7,6} = 8.8$, $J_{7,9} = 2.5$, H-C(7)); 7.46 (d, 1H, $J_{6,7} = 8.8$, H-C(6)). $^{13}\text{C-NMR}$ (CDCl_3 , δ_{C}): 155.16 (s, C(1)); 161.24 (s, C(2)); 111.66 (d, C(3)); 152.46 (s, C(4)); 113.28 (s, C(5)); 125.32 (d, C(6)); 112.55 (d, C(7)); 162.09 (s, C(8)); 101.19 (d, C(9)); 18.53 (q, C(10)); 68.10 (t, C(11)); 26.47 (t, C(12)); 32.88 (t, C(13)); 146.96 (s, C(14)); 116.64 (d, C(15)); 31.13 (t, C(16)); 40.69 (d, C(17)); 37.83 (s, C(18)); 45.60 (d, C(19)); 31.57 (t, C(20)); 26.18 (q, C(21)); 21.06 (q, C(22)).

7-(4-((1R,5S)-6,6-Dimethylbicyclo[3.1.1]hept-2-en-2-yl)butoxy)-4-methyl-2H-chromen-2-one (17f). Yield: 24%, method a. M.p. 77 °C. $[\alpha]_{589}^{26} = -20.3$ ($c = 0.60$, CHCl_3). HRMS: 351.1954 ($[\text{M-H}]^+$, m/z calcd for $\text{C}_{23}\text{H}_{27}\text{O}_3$ 351.1955). $^1\text{H-NMR}$ (CDCl_3 , δ_{H}): 0.81 (s, 3H-C(23)); 1.11 (d, 1H, $^2J = 8.5$, $H_{\text{anti-C(21)}}$); 1.24 (s, 3H-C(22)); 1.43–1.57 (m, 2H, 2H-C(13)); 1.74–1.82 (m, 2H, 2H-C(12)); 1.96–2.02 (m, 3H, 2H-C(14)), 1H-C(20)); 2.03–2.08 (m, 1H, H-C(18)); 2.16 (dm, 1H, $^2J = 17.5$, H-C(17)); 2.23 (dm, 1H, $^2J = 17.5$, H'-C(17)); 2.33 (ddd, 1H, $^2J = 8.5$, $J_{21\text{sin},18} = J_{21\text{sin},20} = 5.6$, $H_{\text{sin-C(21)}}$); 2.37 (d, 3H, $J_{10,3} = 1.2$, 3H-C(10)); 3.98 (t, 2H, $J_{11,12} = 6.5$, 2H-C(11)); 5.16–5.20 (m, 1H, H-C(16)); 6.10 (q, 1H, $J_{3,10} = 1.2$, H-C(3)); 6.77 (d, 1H, $J_{9,7} = 2.5$, H-C(9)); 6.82 (dd, 1H, $J_{7,6} = 8.8$, $J_{7,9} = 2.5$, H-C(7)); 7.45 (d, 1H, $J_{6,7} = 8.8$, H-C(6)). $^{13}\text{C-NMR}$ (CDCl_3 , δ_{C}): 155.14 (s, C(1)); 161.25 (s, C(2)); 111.65 (d, C(3)); 152.46 (s, C(4)); 113.24 (s, C(5)); 125.31 (d, C(6)); 112.53 (d, C(7)); 162.06 (s, C(8)); 101.18 (d, C(9)); 18.55 (q, C(10)); 68.33 (t, C(11)); 28.59 (t, C(12)); 23.33 (t, C(13)); 36.35 (t, C(14)); 147.70 (s, C(15)); 116.13 (d, C(16)); 31.12 (t, C(17)); 40.70 (d, C(18)); 37.80 (s, C(19)); 45.55 (d, C(20)); 31.54 (t, C(21)); 26.20 (q, C(22)); 21.07 (q, C(23)).

7-(3-((1R,5S)-6,6-Dimethylbicyclo[3.1.1]hept-2-en-2-yl)propoxy)-2,3-dihydrocyclopenta[*c*]chromen-4(1H)-one (18e) Yield 47%, method a. M.p. 68 °C. $[\alpha]_{589}^{24.5} = -18.6$ ($c = 0.88$, CHCl_3). HRMS: 364.2038 ($[\text{M}]^+$, m/z calcd for $\text{C}_{24}\text{H}_{28}\text{O}_3$ 364.2033). $^1\text{H-NMR}$ (CDCl_3 , δ_{H}): 0.81 (s, 3H-C(24)); 1.12 (d, 1H, $^2J = 8.5$, $H_{\text{anti-C(22)}}$); 1.25 (s, 3H-C(23)); 1.77–1.90 (m, 2H, 2H-C(14)); 2.01 (ddd, 1 H, $J_{21,19} = J_{21,22\text{sin}} = 5.6$, $J_{21,17} = 1.4$, H-C(21)); 2.04–2.12

(m, 3H, 2H-C(15), 1H-C(19)); 2.13–2.19 (m, 3H, 2H-C(11), 1H-C(18)); 2.23 (dm, 1H, $^2J = 17.6$, H'-C(18)); 2.34 (ddd, 1H, $^2J = 8.5$, $J_{22s,19} = J_{22s,21} = 5.6$, $H_{\text{sin}}\text{-C}(22)$); 2.83–2.88 (m, 2H, 2H-C(10)); 2.98–3.03 (m, 2H, 2H-C(12)); 3.96 (t, 2H, $J_{13,14} = 6.5$, 2H-C(13)); 5.19–5.23 (m, 1H, H-C(17)); 6.78–6.82 (m, 2H, H-C(7), H-C(9)); 7.27–7.32 (m, 1H, H-C(6)). $^{13}\text{C-NMR}$ (CDCl_3 , δ_{C}): 155.64 (s, C(1)); 160.46 (s, C(2)); 124.16 (s, C(3)); 156.28 (s, C(4)); 112.11 (s, C(5)); 125.38 (d, C(6)); 112.45 (d, C(7)); 161.43 (s, C(8)); 101.10 (d, C(9)); 30.20 (t, C(10)); 22.43 (t, C(11)); 31.90 (t, C(12)); 68.04 (t, C(13)); 26.50 (t, C(14)); 32.90 (t, C(15)); 146.99 (s, C(16)); 116.59 (d, C(17)); 31.12 (t, C(18)); 40.68 (d, C(19)); 37.81 (s, C(20)); 45.59 (d, C(21)); 31.56 (t, C(22)); 26.17 (q, C(23)); 21.05 (q, C(24)).

3-(4-((1R,5S)-6,6-Dimethylbicyclo[3.1.1]hept-2-en-2-yl)butoxy)-2,3-dihydrocyclopenta[c]chromen-4(1H)-one (**18f**). Yield: 53%, method a. M.p. 61 °C. $[\alpha]_{589}^{26} = -17.0$ ($c = 1.00$, CHCl_3). HRMS: 377.2110 ($[\text{M-H}]^+$, m/z calcd for $\text{C}_{25}\text{H}_{29}\text{O}_3$ 377.2111). $^1\text{H-NMR}$ (CDCl_3 , δ_{H}): 0.80 (s, 3H-C(25)); 1.11 (d, 1H, $^2J = 8.5$, $H_{\text{anti}}\text{-C}(23)$); 1.24 (s, 3H-C(24)); 1.43–1.56 (m, 2H, 2H-C(15)); 1.73–1.81 (m, 2H, 2H-C(14)); 1.95–2.01 (m, 3H, 2H-C(16), H-C(22)); 2.02–2.07 (m, 1H, H-C(20)); 2.12–2.19 (m, 3H, 2H-C(11), 1H-C(19)); 2.22 (dm, 1H, $^2J = 17.5$, H'-C(19)); 2.32 (ddd, 1H, $^2J = 8.5$, $J_{23\text{sin},20} = J_{23\text{sin},22} = 5.6$, $H_{\text{sin}}\text{-C}(23)$); 2.82–2.88 (m, 2H, 2H-C(10)); 2.97–3.03 (m, 2H, 2H-C(12)); 3.97 (t, 2H, $J_{13,14} = 6.5$, 2H-C(13)); 5.16–5.20 (m, 1H, H-C(18)); 6.78–6.82 (m, 2H, H-C(7), H-C(9)); 7.26–7.32 (m, 1H, H-C(6)). $^{13}\text{C-NMR}$ (CDCl_3 , δ_{C}): 155.62 (s, C(1)); 160.48 (s, C(2)); 124.14 (s, C(3)); 156.29 (s, C(4)); 112.07 (s, C(5)); 125.37 (d, C(6)); 112.42 (d, C(7)); 161.40 (s, C(8)); 101.10 (d, C(9)); 30.19 (t, C(10)); 22.41 (t, C(11)); 31.90 (t, C(12)); 68.26 (t, C(13)); 28.62 (t, C(14)); 23.34 (t, C(15)); 36.35 (t, C(16)); 147.72 (s, C(17)); 116.10 (d, C(18)); 31.11 (t, C(19)); 40.69 (d, C(20)); 37.79 (s, C(21)); 45.54 (d, C(22)); 31.53 (t, C(23)); 26.19 (q, C(24)); 21.06 (q, C(25)).

3-(3-((1R,5S)-6,6-Dimethylbicyclo[3.1.1]hept-2-en-2-yl)propoxy)-7,8,9,10-tetrahydro-6H-benzo[c]chromen-6-one (**19e**). Yield: 33%, method a. M.p. 70 °C. $[\alpha]_{589}^{24.5} = -17.8$ ($c = 0.73$, CHCl_3). HRMS: 377.2110 ($[\text{M-H}]^+$, m/z calcd for $\text{C}_{25}\text{H}_{29}\text{O}_3$ 377.2111). $^1\text{H-NMR}$ (CDCl_3 , δ_{H}): 0.81 (s, 3H-C(25)); 1.12 (d, 1H, $^2J = 8.6$, $H_{\text{anti}}\text{-C}(23)$); 1.25 (s, 3H-C(24)); 1.73–1.89 (m, 6H, 2H-C(11), 2H-C(12), 2H-C(15)); 2.01 (ddd, 1H, $J_{22,20} = J_{22,23\text{sin}} = 5.6$, $J_{22,18} = 1.4$, H-C(22)); 2.04–2.12 (m, 3H, 2H-C(16), 1H-C(20)); 2.16 (dm, 1H, $^2J = 17.5$, H-C(19)); 2.23 (dm, 1H, $^2J = 17.5$, H'-C(19)); 2.34 (ddd, 1H, $^2J = 8.6$, $J_{23\text{sin},20} = J_{23\text{sin},22} = 5.6$, $H_{\text{sin}}\text{-C}(23)$); 2.50–2.55 (m, 2H, 2H-C(10)); 2.69–2.74 (m, 2H, 2H-C(13)); 3.96 (t, 2H, $J_{14,15} = 6.5$, 2H-C(14)); 5.19–5.23 (m, 1H, H-C(18)); 6.75 (d, 1H, $J_{9,7} = 2.5$, H-C(9)); 6.80 (dd, 1H, $J_{7,6} = 8.8$, $J_{7,9} = 2.5$, H-C(7)); 7.41 (d, 1H, $J_{6,7} = 8.8$, H-C(6)). $^{13}\text{C-NMR}$ (CDCl_3 , δ_{C}): 153.38 (s, C(1)); 162.09 (s, C(2)); 120.22 (s, C(3)); 147.19 (s, C(4)); 113.46 (s, C(5)); 123.90 (d, C(6)); 112.23 (d, C(7)); 160.85 (s, C(8)); 100.97 (d, C(9)); 23.69 (t, C(10)); 21.57 (t, C(11)); 21.27 (t, C(12)); 25.08 (t, C(13)); 67.99 (t, C(14)); 26.52 (t, C(15)); 32.91 (t, C(16)); 147.03 (s, C(17)); 116.57 (d, C(18)); 31.13 (t, C(19)); 40.70 (d, C(20)); 37.82 (s, C(21)); 45.61 (d, C(22)); 31.57 (t, C(23)); 26.18 (q, C(24)), 21.06 (q, C(25)).

3-(4-((1R,5S)-6,6-Dimethylbicyclo[3.1.1]hept-2-en-2-yl)butoxy)-7,8,9,10-tetrahydro-6H-benzo[c]chromen-6-one (**19f**). Yield: 36%, method a. M.p. 69 °C. $[\alpha]_{589}^{27} = -17.6$ ($c = 0.90$, CHCl_3). HRMS: 391.2265 ($[\text{M-H}]^+$, m/z calcd for $\text{C}_{26}\text{H}_{31}\text{O}_3$ 391.2268). $^1\text{H-NMR}$ (CDCl_3 , δ_{H}): $^1\text{H-NMR}$ (CDCl_3 , δ_{H}): 0.81 (s, 3H-C(26)); 1.11 (d, 1H, $^2J = 8.5$, $H_{\text{anti}}\text{-C}(24)$); 1.24 (s, 3H-C(25)); 1.42–1.56 (m, 2H, 2H-C(16)); 1.73–1.86 (m, 6H, 2H-C(11), 2H-C(12), 2H-C(15)); 1.95–2.02 (m, 3H, 2H-C(17), H-C(23)); 2.02–2.08 (m, 1H, H-C(21)); 2.16 (dm, 1H, $^2J = 17.4$, H-C(20)); 2.22 (dm, 1H, $^2J = 17.4$, H'-C(20)); 2.33 (ddd, 1H, $^2J = 8.5$, $J_{24\text{sin},21} = J_{24\text{sin},23} = 5.6$, $H_{\text{sin}}\text{-C}(24)$); 2.49–2.55 (m, 2H, 2H-C(10)); 2.68–2.75 (m, 2H, 2H-C(13)); 3.96 (t, 2H, $J_{14,15} = 6.5$, 2H-C(14)); 5.16–5.20 (m, 1H, H-C(19)); 6.75 (d, 1H, $J_{9,7} = 2.5$, H-C(9)); 6.79 (dd, 1H, $J_{7,6} = 8.8$, $J_{7,9} = 2.5$, H-C(7)); 7.41 (d, 1H, $J_{6,7} = 8.8$, H-C(6)). $^{13}\text{C-NMR}$ (CDCl_3 , δ_{C}): 153.36 (s, C(1)); 162.10 (s, C(2)); 120.19 (s, C(3)); 147.19 (s, C(4)); 113.42 (s, C(5)); 123.89 (d, C(6)); 112.19 (d, C(7)); 160.82 (s, C(8)); 100.95 (d, C(9)); 23.68 (t, C(10)); 21.56 (t, C(11)); 21.25 (t, C(12)); 25.08 (t, C(13)); 68.20 (t, C(14)); 28.64 (t, C(15)); 23.35 (t, C(16)); 36.37 (t, C(17)); 147.74 (s, C(18)); 116.09 (d, C(19)); 31.12 (t, C(20)); 40.70 (d, C(21)); 37.80 (s, C(22)); 45.55 (d, C(23)); 31.54 (t, C(24)); 26.20 (q, C(25)), 21.07 (q, C(26)).

3.1.8. Synthesis of 7-aminocoumarins **23** and **24**

7-Aminocoumarins **23** and **24** were synthesized from *m*-aminophenol **20**, in accordance with [37].

Methoxycarbonyl chloride (3.6 mL 47 mmol) was added dropwise to a cooled (5–10 °C) suspension of *m*-aminophenol **20** (4.4 g, 40 mmol) and K₂CO₃ (3.5 g) in 35 mL of ethyl acetate and 3 mL of water, with vigorous stirring. The mixture was stirred for 1 h; then, 10 mL of water was added, and the mixture was stirred for another 3 h. The product was extracted with ethyl acetate. The extracts were washed with water, 1 M H₂SO₄, and brine, dried with Na₂SO₄, and evaporated. The resulting solid was crystallized from benzene to give 5.7 g of **21** (77%).

A mixture of compound **21** (4.6 g, 28 mmol) and 5.5 mL acetoacetic ester was added dropwise to 12 mL H₂SO₄ with vigorous stirring. The mixture was stirred for 2 h and diluted with 50 mL of ice-water. The precipitate was removed by filtration, washed with water, MeOH, and ether, and dried to give 4.0 g of **22** (61%).

A suspension of 2.8 g (12 mmol) of compound **22** in 6 mL of 45% KOH solution was stirred at 90 °C for 0.5 h until the solution formed. The mixture was cooled and diluted with water and acidified with concentrated HCl to pH 5–6. A solution of alkali was added to the suspension, to obtain pH 8. The mixture was stirred until crystallization ceased. The precipitate was removed by filtration, washed with water, MeOH, ether and dried to give 1.53 g of **23** (73%).

Similarly, compound **24** was synthesized from compound **21** with a yield of 64%.

3.1.9. Synthesis of 7-aminocoumarins **25–27**

Amine **25** was obtained by the interaction of compound **23** and (–)-nopinal and subsequent reduction with NaBH₃CN, in accordance with [42].

Compound **25** (0.097 g, 1.0 mmol), (–)-nopinal (0.112 g 1.2 mmol) (synthesized by the oxidation of (–)-nopol with IBX according to the procedure [43]) and acetic acid (100 µL) were dissolved in methanol (5 mL) and stirred at room temperature for 2.5 h. NaBH₃CN (0.110 g, 2.0 mmol) was added, and the reaction mixture was stirred at room temperature for 1.5 h. Methanol was evaporated and the reaction mixture was extracted with CH₂Cl₂. The organic layer was washed with brine, dried over anhydrous Na₂SO₄, filtered, and evaporated. The residue was crystallized from ethanol to give 0.115 g of **25** (64%).

Similarly, compound **27** was synthesized from amine **24** and (–)-myrtenal (yield-57%).

7-N-acetylaminocoumarin **26** was synthesized from 7-aminocoumarin **23**, in accordance with [38].

A mixture of 7-aminocoumarin **23** (0.200 g, 1.1 mmol) and DMAP (20 mg) was dissolved in 1 mL CH₂Cl₂. Acetic anhydride (0.2 mL, 2.1 mmol) was added, and the mixture was stirred at room temperature for 24 h. On completion of the reaction, 10 mL of ice-cold water was added. The precipitate was filtered, washed with water, and dried. The resulting solid was crystallized from ethanol to give 0.176 g of **26** (71%). NMR spectrum **26** coincided with the corresponding spectrum published in the literature [38].

7-(2-((1*R*,5*S*)-6,6-Dimethylbicyclo[3.1.1]hept-2-en-2-yl)ethylamino)-4-methyl-2*H*-chromen-2-one (**25**). Yield: 64% M.p. 131 °C. $[\alpha]_{589}^{27} = -19.7$ ($c = 0.95$, CHCl₃). HRMS: 323.1878 ([M]⁺, m/z calcd for C₂₁H₂₅O₂N₁ 323.1880). ¹H-NMR (CDCl₃, δ_H): 0.81 (s, 3H-C(21)); 1.11 (d, 1H, ²J = 8.6, H_{anti}-C(19)); 1.25 (s, 3H-C(20)); 2.04 (ddd, 1 H, J_{18,16} = J_{18,19sin} = 5.6, J_{18,14} = 1.4, H-C(18)); 2.07–2.11 (m, 1H, H-C(16)); 2.21 (dm, 1H, ²J = 17.6, H-C(15)); 2.25–2.33 (m, 3H, 22H-C(12), 1H'-C(15)); 2.31 (d, 3H, J_{10,3} = 1.2, 3H-C(10)); 2.36 (ddd, 1H, ²J = 8.6, J_{19sin,16} = J_{19sin,18} = 5.6, H_{sin}-C(19)); 3.10–3.19 (m, 2H, 2H-C(11)); 5.32–5.36 (m, 1H, H-C(14)); 5.95 (q, 1H, J_{3,10} = 1.2, H-C(3)); 6.44 (d, 1H, J_{9,7} = 2.4, H-C(9)); 6.49 (dd, 1H, J_{7,6} = 8.7, J_{7,9} = 2.4, H-C(7)); 7.32 (d, 1H, J_{6,7} = 8.7, H-C(6)).

¹³C-NMR (CDCl₃, δ_C): 155.83 (s, C(1)); 161.80 (s, C(2)); 109.39 (d, C(3)); 152.79 (s, C(4)); 110.64 (s, C(5)); 125.34 (d, C(6)); 110.57 (d, C(7)); 150.96 (s, C(8)); 98.32 (d, C(9)); 18.40 (q, C(10)); 40.89 (t, C(11)); 35.79 (t, C(12)); 144.85 (s, C(13)); 119.21 (d, C(14)); 31.24 (t, C(15));

40.59 (d, C(16)); 37.86 (s, C(17)); 45.13 (d, C(18)); 31.64 (t, C(19)); 26.08 (q, C(20)); 21.10 (q, C(21)).

3-(((1R,5S)-6,6-Dimethylbicyclo[3.1.1]hept-2-en-2-yl)methylamino)-7,8,9,10-tetrahydro-6H-benzo[c]chromen-6-one (**27**). Yield: 57%. $[\alpha]_{589}^{27} = -16.3$ ($c = 0.74$, CHCl_3). HRMS: 349.2040 ($[\text{M}]^+$, m/z calcd for $\text{C}_{23}\text{H}_{27}\text{O}_2\text{N}_1$ 349.2036). $^1\text{H-NMR}$ (CDCl_3 , δ_{H}): 0.79 (s, 3H-C(23)); 1.12 (d, 1H, $^2J = 8.6$, $\text{H}_{\text{anti-C(21)}}$); 1.25 (s, 3H-C(22)); 1.71–1.82 (m, 4H, 2H-C(11), 2H-C(12)); 2.05–2.10 (m, 2H, H-C(18), H-C(20)); 2.19 (dm, 1H, $^2J = 17.8$, H-C(17)); 2.26 (dm, 1H, $^2J = 17.8$, H'-C(17)); 2.36 (ddd, 1H, $^2J = 8.6$, $J_{21\text{sin},18} = J_{21\text{sin},20} = 5.6$, $\text{H}_{\text{sin-C(21)}}$); 2.47–2.52 (m, 2H, 2H-C(10)); 2.64–2.70 (m, 2H, 2H-C(13)); 3.62–3.66 (m, 2H, 2H-C(14)); 5.41–5.45 (m, 1H, H-C(16)); 6.45 (d, 1H, $J_{9,7} = 2.4$, H-C(9)); 6.50 (dd, 1H, $J_{7,6} = 8.7$, $J_{7,9} = 2.4$, H-C(7)); 7.28 (d, 1H, $J_{6,7} = 8.7$, H-C(6)). $^{13}\text{C-NMR}$ (CDCl_3 , δ_{C}): 153.92 (s, C(1)); 162.57 (s, C(2)); 117.92 (s, C(3)); 147.63 (s, C(4)); 110.83 (s, C(5)); 123.77 (d, C(6)); 110.51 (d, C(7)); 149.93 (s, C(8)); 98.57 (d, C(9)); 23.62 (t, C(10)); 21.73 (t, C(11)); 21.38 (t, C(12)); 24.99 (t, C(13)); 48.54 (t, C(14)); 144.05 (s, C(15)); 118.81 (d, C(16)); 31.01 (t, C(17)); 40.71 (d, C(18)); 38.00 (s, C(19)); 43.87 (d, C(20)); 31.46 (t, C(21)); 26.01 (q, C(22)), 21.00 (q, C(23)).

3.2. Biology

3.2.1. Cytotoxicity Test

The compounds were weighed in amounts of 2 mg and dissolved in 100 μL of DMSO. Then, the resulting solution was adjusted with the medium to a concentration of 1000 $\mu\text{g}/\text{mL}$, and a series of twofold dilutions was prepared from it. One-day culture of HEp2 cells, grown in 96-well plates, cell concentration 3×10^5 /well of the plate, was checked visually in an inverted microscope for the integrity of the monolayer. Plates were selected for work where the cell closure was 60–80%.

Dilutions of the compounds at the appropriate concentration were added to the plate in a volume of 100 μL in each well in two replicates for each tested concentration. The plates were incubated for 24 h at 37 °C in the presence of 5% CO_2 . Cell viability was assessed using the MTT assay.

The MTT solution was prepared on a maintenance medium at a concentration of 0.5 mg/mL. Then, 0.1 mL of MTT solution was added to each well. After 1.5 h of MTT contact at 37 °C at a CO_2 concentration of 5%, MTT was discarded with the cells of the well and 0.1 mL of ethyl alcohol 96% was poured, after which the optical density in the wells was measured at a wavelength of 535 nm. Based on the data obtained, the CC_{50} was calculated.

3.2.2. Antiviral Activity

The antiviral activity against the respiratory syncytial virus (RSV A—strain A2, RSV B—strain 9320) was assessed in a series of threefold dilutions of test compounds, starting from $\frac{1}{2}\text{CC}_{50}$, which were added to HEp-2 cell culture at a double concentration, at 100 μL per well, followed by the addition of 100 μL of the virus in a series of 10-fold dilutions. Cells were incubated at 37 °C and 5% CO_2 for 1 h. Then, the virus was washed out, and the compounds were again added at a single concentration and incubated at 37 °C and 5% CO_2 for 6 days. For the enzyme-linked immunosorbent assay (ELISA), cell culture was fixed with cold 80% acetone at -20 °C for 15 min and then washed with phosphate-buffered saline containing 0.05% Tween 20. Next, a solution of primary mouse anti-RSV F protein antibodies was added to the culture and incubated at room temperature under continuous stirring for 2 h. Then, cells were again washed with buffer, secondary anti-mouse antibodies were added, and the cells were incubated under continuous stirring for 2 h. Then, the antibodies were washed off, and a substrate–chromogenic mixture with tetramethylbenzidine was added. After 5 min, the reaction was stopped with 0.1 M sulfuric acid, and the optical density of the solution was measured at a wavelength of 450 nm. Wells with absorbance values twofold or greater than the cell control were considered contaminated. The virus titer was calculated using the Reed and Muench method. All experiments were made in triplicate.

3.2.3. Time-of-Addition Assay

Compound **19c** was added at different time points before, after or simultaneously with the introduction of the virus. The time of addition of the compound was counted from point 0—the time of entry of the virus into the cell. During the period (−1)–0, the cells together with the virus were incubated at 40 °C. All other experiments were carried out at 37 °C. RSV virus A 2 mL was added to the cells at a time that was conventionally designated as point −1, after which the cells were kept for an hour at a temperature of 40 °C. Then, at point 0, the virus was unbound. The cells were transferred to a thermostat at 37 °C, where they were incubated for 25 h. After this period, the medium was taken from each well and a series of ten-fold dilutions were made on a fresh cell culture and incubated for 6 days. For each compound, 2 repetitions were made by different operators. The virus titer was estimated by ELISA. The compound was added at the following times relative to the addition of the virus: point −2—the compound was introduced one hour before cell infection (prophylactic regimen); point 0—at the moment of temperature change; points 1, 2, 4, 6, 24—after 1, 2, 4, 6 and 24 h after the temperature change, respectively. In the wells marked (−2) – (25), the compound was kept throughout the experiment, starting from point −2 and until the end of the experiment −25 h. No compound was added to the control wells; instead, a similar volume of medium was added.

3.3. Molecular Modeling

3.3.1. Receptor and Ligand Preparation

Crystallographic structures of the RSV F protein (PDB codes 7LVW [39] and 7KQD [15]) were downloaded from the Protein Data Bank database [40]. The code of the full-length protein trimer was 7LVW; 7KQD is the code of a ligand–protein complex, but only one protein from three trimeric forms. Model protein structures were prepared using the Schrodinger Protein Preparation Wizard tool (Schrodinger Suite Software): hydrogen atoms were added and minimized; missing amino acid side chains were added; bond multiplicities were restored; solvent molecules were removed; and the entire structure was optimized in the OPLS3e force field [44] at a physiological pH value. For a correct calculation procedure, we used binding site alignment procedures 7LVW and 7KQD. As results, full-size proteins and ligands (sisunatovir) in complex were obtained.

The geometric parameters of ligands (coumarin derivatives) and sisunatovir (RSV F inhibitor) were also optimized, taking into account all permissible conformations.

3.3.2. Molecular Docking

Molecular docking was performed using Schrodinger Suite (Release 2020-4) software. Coumarin derivatives were docked using the forced ligand positioning protocol (IFD) under the following conditions: flexible protein and ligand; grid matrix size of 15 Å; and amino acids (within a radius of 5 Å from the ligand) restrained and optimized, taking into account the influence of a ligand. Docking solutions were ranked by evaluating the following calculation parameters: docking score (based on GlideScore minus penalties); ligand efficiency (LE, which takes into account an atomic distribution of the scoring function); a model energy value (E_{model}), including a GlideScore value, energy-unrelated interactions, and parameters of the energy spent in positioning of the ligand in the binding site.

Supplementary Materials: NMR ¹H and ¹³C spectra of compounds **16–19**, **25**, and **27**; Energy parameters of the docking study procedure; Figure S1—best position of Sisunatovir; Figure S2—best position of **19c**; Figure S3—best position of **19f**; Figure S4—best position of **19h**; Figure S5—the pharmacophore features of known F-protein inhibitor of sisunatovir and compounds **19c**, **19f**, and **19h**; 1. Figure S6—Dose-response curve and half maximal inhibitory concentration (IC₅₀) values of active compounds in Hep-2 cells against RSV A and B. Table S1—Energy parameters of docking study procedure.

Author Contributions: Conceptualization, N.F.S., A.A.S., and K.P.V.; methodology, N.F.S., A.A.S., S.S.B., and K.P.V.; investigation, T.M.K., A.A.S., A.V.G., Y.V.N., G.D.P., S.S.B., and D.V.K.; writing—original draft preparation, T.M.K., A.A.S., S.S.B., and K.P.V.; writing—review and editing, N.F.S.; supervision, N.F.S.; project administration, K.P.V. All authors have read and agreed to the published version of the manuscript.

Funding: This study was funded by the Russian Science Foundation (Moscow, Russia) grant 21-13-00026.

Institutional Review Board Statement: Not applicable.

Informed Consent Statement: Not applicable.

Data Availability Statement: The data presented in this study are available on request from the corresponding author.

Acknowledgments: The authors would like to acknowledge the Multi-Access Chemical Research Center SB RAS for spectral and analytical measurements.

Conflicts of Interest: The funders had no role in the design of the study; in the collection, analyses, or interpretation of data; in the writing of the manuscript, or in the decision to publish the results.

Sample Availability: Samples of the compounds presented in this study are available on request from the authors.

References

1. Afonso, C.L.; Amarasinghe, G.K.; Bányai, K.; Bào, Y.; Basler, C.F.; Bavari, S.; Bejerman, N.; Blasdel, K.R.; Briand, F.; Briesse, T.; et al. Taxonomy of the order Mononegavirales: Update 2016. *Arch. Virol.* **2016**, *161*, 2351–2360. [CrossRef] [PubMed]
2. Karron, R.A. Preventing respiratory syncytial virus (RSV) disease in children. *Science* **2021**, *372*, 686–687. [CrossRef] [PubMed]
3. Lozano, R.; Naghavi, M.; Foreman, K.; Lim, S.; Shibuya, K.; Aboyans, V.; Abraham, J.; Adair, T.; Aggarwal, R.; Ahn, S.Y.; et al. Global and regional mortality from 235 causes of death for 20 age groups in 1990 and 2010: A systematic analysis for the Global Burden of Disease Study 2010. *Lancet* **2012**, *380*, 2095–2128. [CrossRef]
4. Falsey, A.R.; Hennessey, P.A.; Formica, M.A.; Cox, C.; Walsh, E.E. Respiratory syncytial virus infection in elderly and high-risk adults. *N. Engl. J. Med.* **2005**, *352*, 1749–1759. [CrossRef] [PubMed]
5. Huang, H.; Chen, S.; Zhang, X.; Hong, L.; Zeng, Y.; Wu, B. Detection and clinical characteristics analysis of respiratory viruses in hospitalized children with acute respiratory tract infections by a GeXP-based multiplex-PCR assay. *J. Clin. Lab. Anal.* **2020**, *34*, e23127. [CrossRef]
6. Nair, H.; Nokes, D.J.; Gessner, B.D.; Dherani, M.; Madhi, S.A.; Singleton, R.J.; O'Brien, K.L.; Roca, A.; Wright, P.F.; Bruce, N.; et al. Global burden of acute lower respiratory infections due to respiratory syncytial virus in young children: A systematic review and meta-analysis. *Lancet* **2010**, *375*, 1545–1555. [CrossRef]
7. Available online: <http://www.pharmafile.com/news/583523/parents-warned-child-respiratory-illness-rise-summer> (accessed on 20 September 2021).
8. Wainwright, C. Acute viral bronchiolitis in children—A very common condition with few therapeutic options. *Paediatr. Respir. Rev.* **2010**, *11*, 39–45. [CrossRef] [PubMed]
9. Empey, K.M.; Peebles, R.S., Jr.; Kolls, J.K. Pharmacologic advances in the treatment and prevention of respiratory syncytial virus. *Clin. Infect. Dis.* **2010**, *50*, 1258–1267. [CrossRef] [PubMed]
10. Cockerill, G.S.; Good, J.A.D.; Mathews, N. State of the Art in Respiratory Syncytial Virus Drug Discovery and Development. *J. Med. Chem.* **2019**, *62*, 3206–3227. [CrossRef] [PubMed]
11. Nikolayeva, Y.V.; Ulashchik, E.A.; Chekerda, E.V.; Galochkina, A.V.; Slesarchuk, N.A.; Chistov, A.A.; Nikitin, T.D.; Korshun, V.A.; Shmanai, V.V.; Ustinov, A.V.; et al. 5-(Perylen-3-ylethynyl)uracil Derivatives Inhibit Reproduction of Respiratory Viruses. *Russ. J. Bioorg. Chem.* **2020**, *46*, 315–320. [CrossRef]
12. Huo, X.; Hou, D.; Wang, H.; He, B.; Fang, J.; Meng, Y.; Liu, L.; Wei, Z.; Wang, Z.; Liu, F.-W. Design, synthesis, in vitro and in vivo anti-respiratory syncytial virus (RSV) activity of novel oxizine fused benzimidazole derivatives. *Eur. J. Med. Chem.* **2021**, *224*, 113684. [CrossRef]
13. Xu, J.; Wu, W.; Chen, H.; Xue, Y.; Bao, X.; Zhou, J. Substituted N-(4-amino-2-chlorophenyl)-5-chloro-2-hydroxybenzamide analogues potently inhibit respiratory syncytial virus (RSV) replication and RSV infection-associated inflammatory responses. *Bioorg. Med. Chem.* **2021**, *39*, 116157. [CrossRef]
14. Vendeville, S.; Tahri, A.; Hu, L.; Demin, S.; Coymans, L.; Vos, A.; Kwanten, L.; Van den Berg, J.; Battles, M.B.; McLellan, J.S.; et al. Discovery of 3-((5-Chloro-1-[3-(methylsulfonyl)propyl]-1H-indol-2-yl)methyl)-1-(2,2,2-trifluoroethyl)-1,3-dihydro-2H-imidazo[4,5-c]pyridin-2-one (JNJ-53718678), a Potent and Orally Bioavailable Fusion Inhibitor of Respiratory Syncytial Virus. *J. Med. Chem.* **2020**, *63*, 8046–8058. [CrossRef]

15. Cockerill, G.S.; Angell, R.M.; Bedernjak, A.; Chuckowree, I.; Fraser, I.; Gascon-Simorte, J.; Gilman, M.S.A.; Good, J.A.D.; Harland, R.; Johnson, S.M.; et al. Discovery of Sisunatovir (RV521), an Inhibitor of Respiratory Syncytial Virus Fusion. *J. Med. Chem.* **2021**, *64*, 3658–3676. [[CrossRef](#)] [[PubMed](#)]
16. Annunziata, F.; Pinna, C.; Dallavalle, S.; Tamborini, L.; Pinto, A. An Overview of Coumarin as a Versatile and Readily Accessible Scaffold with Broad-Ranging Biological Activities. *Int. J. Mol. Sci.* **2020**, *21*, 4618. [[CrossRef](#)] [[PubMed](#)]
17. Khomenko, T.M.; Zakharenko, A.L.; Chepanova, A.A.; Ilina, E.S.; Zakharova, O.D.; Kaledin, V.I.; Nikolin, V.P.; Popova, N.A.; Korchagina, D.V.; Reynisson, J.; et al. New Promising Inhibitors of Tyrosyl-DNA Phosphodiesterase I (Tdp 1) Combining 4-Arylcoumarin and Monoterpenoid Moieties as Components of Complex Antitumor Therapy. *Int. J. Mol. Sci.* **2020**, *21*, 126. [[CrossRef](#)] [[PubMed](#)]
18. Al-Warhi, T.; Sabt, A.; Elkaeed, E.B.; Eldehna, W.M. Recent advancements of coumarin-based anticancer agents: An up-to-date review. *Bioorg. Chem.* **2020**, *103*, 104163. [[CrossRef](#)] [[PubMed](#)]
19. Küpeli Akkol, E.; Genç, Y.; Karpuz, B.; Sobarzo-Sánchez, E.; Capasso, R. Coumarins and Coumarin-Related Compounds in Pharmacotherapy of Cancer. *Cancers* **2020**, *12*, 1959. [[CrossRef](#)] [[PubMed](#)]
20. Carneiro, A.; Matos, M.J.; Uriarte, E.; Santana, L. Trending Topics on Coumarin and Its Derivatives in 2020. *Molecules* **2021**, *26*, 501. [[CrossRef](#)] [[PubMed](#)]
21. Mishra, S.; Pandey, A.; Manvati, S. Coumarin: An emerging antiviral agent. *Heliyon* **2020**, *6*, e03217. [[CrossRef](#)] [[PubMed](#)]
22. Gao, Y.; Cheng, H.; Khan, S.; Xiao, G.; Rong, L.; Bai, C. Development of coumarine derivatives as potent anti-filovirus entry inhibitors targeting viral glycoprotein. *Eur. J. Med. Chem.* **2020**, *204*, 112595. [[CrossRef](#)]
23. Zhong, Z.J.; Cheng, L.P.; Pang, W.; Zheng, X.S.; Fu, S.K. Design, synthesis and biological evaluation of dihydrofurocoumarin derivatives as potent neuraminidase inhibitors. *Bioorg. Med. Chem. Lett.* **2021**, *37*, 127839. [[CrossRef](#)] [[PubMed](#)]
24. Lai, Y.; Han, T.; Zhan, S.; Jiang, Y.; Liu, X.; Li, G. Antiviral Activity of Isoimperatorin against Influenza A Virus in vitro and its Inhibition of Neuraminidase. *Front. Pharmacol.* **2021**, *12*, 65782. [[CrossRef](#)] [[PubMed](#)]
25. Li, Z.; Kong, D.; Liu, Y.; Liu, Y.; Li, M. Pharmacological perspectives and molecular mechanisms of coumarin derivatives against virus disease. *Genes Dis.* **2021**. [[CrossRef](#)]
26. Hu, Y.; Shan, L.; Qiu, T.; Liu, L.; Chen, J. Synthesis and biological evaluation of novel coumarin derivatives in rhabdoviral clearance. *Eur. J. Med. Chem.* **2021**, *223*, 113739. [[CrossRef](#)]
27. Mazzei, M.; Nieddu, E.; Miele, M.; Balbi, A.; Ferrone, M.; Fermeglia, M.; Mazzei, M.T.; Prich, S.; La Colla, P.; Marongiu, F.; et al. Activity of Mannich bases of 7-hydroxycoumarin against Flaviviridae. *Bioorg. Med. Chem.* **2008**, *16*, 2591–2605. [[CrossRef](#)] [[PubMed](#)]
28. Yarovaya, O.I.; Salakhutdinov, N.F. Mono- and sesquiterpenes as a starting platform for the development of antiviral drugs. *Russ. Chem. Rev.* **2021**, *90*, 488–510. [[CrossRef](#)]
29. Salakhutdinov, N.F.; Volcho, K.P.; Yarovaya, O.I. Monoterpenes as a renewable source of biologically active compounds. *Pure Appl. Chem.* **2017**, *89*, 1105–1117. [[CrossRef](#)]
30. Khomenko, T.M.; Zarubae, V.V.; Orshanskaya, I.R.; Kadyrova, R.A.; Sannikova, V.A.; Korchagina, D.V.; Volcho, K.P.; Salakhutdinov, N.F. Anti-influenza activity of monoterpene-containing substituted coumarins. *Bioorg. Med. Chem. Lett.* **2017**, *27*, 2920–2925. [[CrossRef](#)]
31. Khomenko, T.; Zakharenko, A.; Odarchenko, T.; Arabshahi, H.J.; Sannikova, V.; Zakharova, O.; Korchagina, D.; Reynisson, J.; Volcho, K.; Salakhutdinov, N.; et al. New inhibitors of tyrosyl-DNA phosphodiesterase I (Tdp 1) combining 7-hydroxycoumarin and monoterpenoid moieties. *Bioorg. Med. Chem.* **2016**, *24*, 5573–5581. [[CrossRef](#)]
32. Akgun, B.; Hall, D.G. Fast and tight boronate formation for click bioorthogonal conjugation. *Angew. Chem. Int. Ed.* **2016**, *55*, 3909–3913. [[CrossRef](#)] [[PubMed](#)]
33. Il'ina, I.V.; Volcho, K.P.; Korchagina, D.V.; Barkhash, V.A.; Salakhutdinov, N.F. Reactions of Allyl Alcohols of the Pinane Series and of Their Epoxides in the Presence of Montmorillonite Clay. *Helv. Chim. Acta* **2007**, *90*, 353–368. [[CrossRef](#)]
34. Chapuis, C.; Brauchli, R. Preparation of campholenal analogues: Chirons for the lipophilic moiety of sandalwood-like odorant alcohols. *Helv. Chim. Acta* **1992**, *75*, 1527–1546. [[CrossRef](#)]
35. Cointeaux, L.; Berrien, J.-F.; Mayrargue, J. Synthesis of cardamom peroxide analogues by radical cyclization of hydroperoxyalkenes. *Tetrahedron Lett.* **2002**, *43*, 6275–6277. [[CrossRef](#)]
36. Pozdnev, V.F. Improved method for synthesis of 7-amino-4-methylcoumarin. *Chem. Heterocycl. Compd.* **1990**, *26*, 264–265. [[CrossRef](#)]
37. Kathuria, A.; Priya, N.; Chand, K.; Singh, P.; Gupta, A.; Jalal, S.; Gupta, S.; Raj, H.G.; Sharma, S.K. Substrate specificity of acetoxy derivatives of coumarins and quinolones towards Calreticulin mediated transacetylation: Investigations on antiplatelet function. *Bioorg. Med. Chem.* **2012**, *20*, 1624–1638. [[CrossRef](#)]
38. Collins, P.L.; Fearn, R.; Graham, B.S. Respiratory Syncytial Virus: Virology, Reverse Genetics, and Pathogenesis of Disease. In *Challenges and Opportunities for Respiratory Syncytial Virus Vaccines*; Anderson, L., Graham, B., Eds.; Current Topics in Microbiology and Immunology; Springer: Berlin/Heidelberg, Germany, 2013; Volume 372. [[CrossRef](#)]
39. Rossey, I.; Hsieh, C.-L.; Sedeyn, K.; Balleger, M.; Schepens, B.; McLellan, J.S.; Saelens, X. A vulnerable, membrane-proximal site in human respiratory syncytial virus F revealed by a prefusion-specific single-domain antibody. *J. Virol.* **2021**, *95*, e02279–20. [[CrossRef](#)] [[PubMed](#)]

40. Berman, H.M.; Westbrook, J.; Feng, Z.; Gilliland, G.; Bhat, T.N.; Weissig, H.; Shindyalov, I.N.; Bourne, P.E. The Protein Data Bank. *Nucleic Acids Res.* **2000**, *28*, 235–242. [[CrossRef](#)] [[PubMed](#)]
41. Kiesgen de Richter, R.; Bonato, M.; Follet, M.; Kamenka, J.M. The (+)- and (–)-[2-(1,3-dithianyl0]myrtanylborane. Solid and stable monoalkylboranes for asymmetric hydroboration. *J. Org. Chem.* **1990**, *55*, 2855–2860. [[CrossRef](#)]
42. El-Haggar, R.; Al-Wabli, R.I. Anti-inflammatory screening and molecular modeling of some novel coumarin derivatives. *Molecules* **2015**, *20*, 5374–5391. [[CrossRef](#)] [[PubMed](#)]
43. Ponomarev, K.; Pavlova, A.; Suslov, E.; Ardashov, O.; Korchagina, D.; Nefedov, A.; Tolstikova, T.; Volcho, K.; Salakhutdinov, N. Synthesis and analgesic activity of new compounds combining azaadamantane and monoterpene moieties. *Med. Chem. Res.* **2015**, *24*, 4146–4156. [[CrossRef](#)]
44. Shivakumar, D.; Harder, E.; Damm, W.; Friesner, R.A.; Sherman, W. Improving the Prediction of Absolute Solvation Free Energies Using the Next Generation OPLS Force Field. *J. Chem. Theory Comput.* **2012**, *8*, 2553–2558. [[CrossRef](#)] [[PubMed](#)]